

A multifrequency characterization of the extragalactic hard X-ray sky

Presenting the 2nd release of the Turin-SyCAT

M. Kosiba^{1,2}, H. A. Peña-Herazo³, F. Massaro^{2,4,5}, N. Masetti^{6,7}, A. Paggi^{2,3,4},
V. Chavushyan⁸, E. Bottacini^{9,10}, and N. Werner¹

¹ Department of Theoretical Physics and Astrophysics, Faculty of Science, Masaryk University, Kotlářská 2, Brno, 611 37, Czech Republic

² Dipartimento di Fisica, Università degli Studi di Torino, via Pietro Giuria 1, I-10125 Torino, Italy.

³ East Asian Observatory, 660 North A'ohōkū Place, Hilo, Hawaii 96720, USA.

⁴ Istituto Nazionale di Fisica Nucleare, Sezione di Torino, I-10125 Torino, Italy

⁵ INAF-Osservatorio Astrofisico di Torino, via Osservatorio 20, I-10025 Pino Torinese, Italy

⁶ INAF - Osservatorio di Astrofisica e Scienza dello Spazio, via Piero Gobetti 101, 40129 Bologna, Italy

⁷ Departamento de Ciencias Físicas, Universidad Andrés Bello, Fernández Concha 700, Las Condes, Santiago, Chile

⁸ Instituto Nacional de Astrofísica, Óptica y Electrónica, Apartado Postal 51-216, 72000 Puebla, México.

⁹ Dipartimento di Fisica e Astronomia G. Galilei, Univeristà di Padova, Padova, Italy.

¹⁰ Eureka Scientific, 2452 Delmer Street Suite 100, Oakland, CA 94602-3017, USA.

Received Month Day, Year; accepted Month Day, Year

ABSTRACT

Context. Nowadays we know that the origin of the Cosmic X-ray Background (CXB) is due to the integrated emission of nearby active galactic nuclei. Thus to obtain a precise estimate of the contribution of different source classes to the CXB it is crucial to have a full characterization of the hard X-ray sky.

Aims. We present a multifrequency analysis of all sources listed in the 3rd release of the Palermo *Swift*-BAT hard X-ray catalog (3PBC) with the goal of (i) identifying and classifying the largest number of sources adopting multifrequency criteria, with particular emphasis on extragalactic populations and (ii) extracting sources belonging to the class of Seyfert galaxies to present here the release of the 2nd version of the Turin-SyCAT.

Methods. We outline a classification scheme based on radio, infrared and optical criteria that allows us to distinguish between unidentified and unclassified hard X-ray sources, as well as to classify those sources belonging to the Galactic and the extragalactic populations.

Results. Our revised version of the 3PBC lists 1176 classified, 820 extragalactic, and 356 Galactic ones, 199 unclassified, and 218 unidentified sources. According to our analysis, the hard X-ray sky is mainly populated by Seyfert galaxies and blazars. For the blazar population, we report trends between the hard X-ray and the gamma-ray emissions since a large fraction of them have also a counterpart detected by the *Fermi* satellite. These trends are all in agreement with the expectations of inverse Compton models widely adopted to explain the blazar broadband emission. For the Seyfert galaxies, we present the 2nd version of the Turin-SyCAT including a total of 633 Seyfert galaxies, with 282 new sources corresponding to an increase by $\sim 80\%$ with respect to the previous release. Comparing the hard X-ray and the infrared emissions of Seyfert galaxies we confirm, that there is no clear difference between the flux distribution of the infrared-to-hard X-ray flux ratio of Seyfert galaxies Type 1 and Type 2. However, there is a significant trend between the mid-IR flux and hard X-ray flux, confirming previous statistical results in the literature.

Conclusions. We provide two catalog tables. The first is the revised version of the 3PBC catalog based on our multifrequency analyses. The second catalog table is a release of the second version of the Turin-SyCAT catalog. Finally, we highlight that the SWIFT archive has already extensive soft X-ray data available to search for potential counterparts of unidentified hard X-ray sources. All these datasets will be reduced and analyzed in a forthcoming analysis to determine the precise position of low energy counterparts in the 0.5 – 10 keV energy range for 3PBC sources that can be targets of future optical spectroscopic campaigns, necessary to obtain their precise classification.

Key words. catalogs – methods: data analyses – X-rays: general

1. Introduction

The Cosmic X-ray background (CXB) was discovered when the earliest X-ray astronomical rocket experiments were carried out (see e.g. Giacconi et al. 1962). It appeared as a diffuse component of X-ray radiation distributed in all directions. In the last decades, after its discovery, several different scenarios were pro-

posed to interpret its origin, such as considering spanning new types of faint discrete X-ray sources whose integrated emission could be responsible for the CXB (e.g. (Gilli et al. 1999), Gilli et al. (2001)) up to diffuse radiative processes occurring in the intergalactic space, as for example exotic emission from dark matter particle decay (see e.g. Abazajian et al. 2001). However, the solution to this puzzle arose thanks to deep images obtained

first with the ROentgen SATellite *ROSAT* (Hasinger et al. 1999), collected in the early ninety's, and more recently with *Chandra* X-ray telescope (Weisskopf et al. 2000), all revealing that about 80 % of CXB is resolved (Hasinger et al. 1998), between 0.5 keV and 2 keV, as suggested by (Cavaliere & Setti 1976). At hard X-ray energies the fraction of resolved CXB by *Swift* and *INTEGRAL* is of 2% (Bottacini et al. 2012) and by *NuSTAR* is of 35% (Harrison et al. 2016). Thus, the origin of the CXB is nowadays established to be mainly due to the high energy emission of the extragalactic discrete sources, whose large fraction belongs to different classes of active galactic nuclei (AGNs) (Gilli et al. 2007).

The first survey in the hard X-ray band was carried by the *UHURU* satellite (a.k.a SAS-1 Giacconi et al. 1971). Since the discovery of the CXB, many surveys were performed in the soft and hard X-ray bands, including Forman et al. (1978) who produced a catalog of 339 X-ray sources observed by the *UHURU* satellite in the 2–20 keV energy band. Levine et al. (1984), using the X-ray and Gamma-ray detector HEAO-A4 on board the *HEAO 1* satellite (Rothschild et al. 1979) presented an all-sky survey in 13–180 keV range detecting 77 new sources. The hard X-ray component of the CXB radiation, observable between 3 keV and up to 300 keV, shows a distinct peak at ~ 30 keV (Gruber et al. 1999) being extremely uniform across the sky with the only exception of an overdensity along the Galactic plane (Valinia & Marshall 1998; Revnitsev et al. 2006; ?) and it is again strictly connected with AGN population emitting in the hard X-rays (Frontera et al. 2007).

The currently flying satellites as the INTERnational Gamma-Ray Astrophysics Laboratory *INTEGRAL* (Winkler et al. 2003), with its Imager on Board the *INTEGRAL* Satellite *IBIS* (Ubertini et al. 2003) and Neil Gehrels *Swift* Observatory (Gehrels et al. 2004) with its Burst Alert Telescope (BAT Barthelmy 2004) on board, carrying measurements in the hard X-rays significantly improved our understanding of the origin of the CXB and refined its measurement. The observed spectrum of the CXB is currently well described by the standard population synthesis model of AGNs, including the fraction of Compton-thick AGNs and the reflection strengths from the accretion disk and torus based on the luminosity- and redshift-dependent unified scheme (Ajello et al. 2008; Ueda et al. 2014). This is shown also in recent results achieved thanks to the *NuSTAR* observations in the 3–20 keV band (Krivonos et al. 2021a). This has been also possible thanks to improvements achieved in the preparation of hard X-ray source catalogues (see e.g. Markwardt et al. 2005; Beckmann et al. 2006; Churazov et al. 2007; ?; Sazonov et al. 2007; Tueller et al. 2008; Cusumano et al. 2010; Bottacini et al. 2012; Bird et al. 2016; Mereminskiy et al. 2016; Krivonos et al. 2017; Oh et al. 2018; Krivonos et al. 2021b, 2022) and the association of hard X-ray sources with their low energy counterparts (e.g. Malizia et al. 2010; Koss et al. 2019; Bär et al. 2019; Smith et al. 2020) and their optical spectroscopy follow-ups (e.g. Masetti et al. 2008, 2012, 2013; Parisi et al. 2014; Rojas et al. 2017; Marchesini et al. 2019).

There are three major catalogues built on observations collected in the last decade with two major space missions still active: (i) the Palermo *Swift*-BAT hard X-ray catalogue (Cusumano et al. 2010) based on 54 months of the *Swift*-BAT operation, currently updated to its 3rd release and with a 4th release ongoing¹, (ii) the *Swift*-BAT all-sky hard X-ray survey, that published the 105 month *Swift*-BAT catalogue (see e.g. Oh et al. 2018), and (iii) the *INTEGRAL* *IBIS* catalogue in the energy range 17–100

keV (Bird et al. 2016), performed using the *INTEGRAL* Soft γ -ray Imager (ISGRI) (Lebrun et al. 2003), the low energy CdTe γ -ray detector on (*IBIS*) telescope (Ubertini et al. 2003).

Here we focus on the investigation of the 3rd release of the Palermo *Swift*-BAT hard X-ray catalog (hereinafter 3PBC), with particular emphasis on extragalactic sources, since the release of the next version is currently ongoing, thus results provided by our analysis could be used therein. The 3PBC is based on the data reduction and detection algorithms of the first Palermo *Swift*-BAT Catalog hard X-ray catalog (Segreto et al. 2010; Cusumano et al. 2010). The 3PBC is available only online² thus we point for the reference the publication of its 2nd release, the 2PBC (Cusumano et al. 2010). The 2PBC provides data in three energy bands, namely: 15 – 30 keV, 15 – 70 keV, 15 – 150 keV for a total of 1256 sources above 4.8 σ level of significance, where 1079 hard X-ray sources have an assigned soft X-ray counterpart, while the remaining 177 are still unassociated. The total source number increased in 3PBC to 1593 when considering a signal-to-noise ratio above 3.8, which is the catalog release we analyzed here. Please note, that only three 3PBC sources are detected at a signal-to-noise ratio lower than 5. The 3PBC catalogue covers 90 % of the sky down to a flux limit of 1.1×10^{-11} erg cm⁻² s⁻¹, decreasing to ~ 50 % when decreasing the flux limit to 0.9×10^{-11} erg cm⁻² s⁻¹.

First, we verified source classification for all associated counterparts listed in the 3PBC, adopting a multifrequency approach. This analysis was corroborated by checking if additional studies, available in the literature and carried out after the last 3PBC release, allowed us to obtain a more complete overview of source populations emitting in the hard X-rays. Then, our final goal was to explore in detail those extragalactic sources being identified as Seyfert galaxies (Antonucci & Miller 1985) to (i) release the 2nd version of the Turin-SyCAT (Peña-Herazo et al. 2022) and thus (ii) refine our statistical analysis on the correlation found between the infrared (IR) and the hard X-ray fluxes for this extragalactic population. Additionally, we also aim at investigating possible connections between the hard X-ray and the gamma-ray emission in those blazars detected by Fermi-LAT. It is worth noting that given our final aim, the classification task performed on the Galactic sources is mainly devoted to excluding them from the final sample of new Seyfert galaxies.

The present work will be also relevant for the association of hard X-ray sources with their low energy counterpart, which will be included in the next releases of hard X-ray catalogs. In addition, we highlight that the proposed investigation will also provide a more complete overview of those sources, that lack an assigned low energy counterpart as still unidentified.

Finally, we remark that the reason underlying the choice of working with the 3PBC rather than subsequent versions of hard X-ray catalogs is mainly motivated by the opportunity of having more multifrequency information available in the literature. However a comparison with other recent catalogues as: the 105 month *Swift*-BAT catalog³ (Oh et al. 2018) and the *INTEGRAL* hard X-ray catalogue (Bird et al. 2016) are also included in the present analysis.

The structure of the paper is outlined as follows: in Section 2, we described various catalogs and surveys used to search for multifrequency information related to high and low energy counterparts of hard X-ray sources; in Section 3, we present our multifrequency classification scheme adopted to label source counterparts. Then Section 4 focuses on the main results of the

² http://bat.ifc.inaf.it/bat_catalog_web/66m_bat_catalog.html

³ <https://heasarc.gsfc.nasa.gov/W3Browse/swift/swbat105m.html>

¹ <https://www.ssdsc.asi.it/bat54/>

characterization of the extragalactic hard X-ray sources while Section 5 is entirely devoted to the second release of the Turin-SyCAT catalog and the statistical analysis for the IR – hard X-ray connection. Finally, our summary, conclusions, and future perspectives are given in Section 6. A comparison between our classification analysis and the previous one of the 3PBC is then reported in Appendix A.

We used cgs units unless stated otherwise. We adopted Λ CDM cosmology with $\Omega_M = 0.286$, and Hubble constant $H_0 = 69.6 \text{ km s}^{-1} \text{ Mpc}^{-1}$ (Bennett et al. 2014) to compute cosmological corrections, the same used for the 1st release of the Turin-SyCAT (Peña-Herazo et al. 2022). WISE magnitudes are in the Vega system and are not corrected for the Galactic extinction. As shown in our previous analyses (D’Abrusco et al. 2014; Massaro & D’Abrusco 2016; D’Abrusco et al. 2019), such correction affects mainly the magnitude at $3.4 \mu\text{m}$ for sources lying at low Galactic latitudes (i.e., $|b| < 20^\circ$), and it ranges between 2% and 5% of their magnitude values, thus not significantly affect our results. We indicate the WISE magnitudes at $3.4, 4.6, 12,$ and $22 \mu\text{m}$ as W1, W2, W3, and W4, respectively. For all WISE magnitudes of sources flagged as extended in the AllWISE catalog (i.e., extended flag “ext_flg” greater than 0) we used values measured in the elliptical aperture. Sloan Digital Sky Survey (SDSS) (Blanton et al. 2017; Abdurro’uf et al. 2021) and Panoramic Survey Telescope & Rapid Response System (Pan-STARRS) (Chambers et al. 2016) magnitudes are in the AB system. Given the large number of acronyms used here, mostly due to different classifications and telescopes used, we summarized them in Table 1.

Table 1. Table of Acronyms used in the text.

Acronym	Meaning
ATNF	australian telescope national facility
CXB	cosmic X-ray background
AGN	active galactic nuclei
BLL	BL-Lac object
BZG	Galaxy Dominated Blazars
BZU	blazar of uncertain type
CV	cataclysmic variable
FSRQ	flat spectrum radio quasar
HERG	high excitation radio galaxy
LERG	low excitation radio galaxy
LINER	Low-ionization nuclear emission-line region galaxy
NOV	novae
PN	planetary nebulae
PSR	pulsar
QSO	quasi stellar objects
RDG	radio galaxy
SNR	supernovae remnant
WD	white dwarf
XBONG	X-ray bright optically normal galaxy

2. Hunting Counterparts of Hard X-ray Sources: Catalogues and Surveys

This section provides a basic overview of all major catalogs used to carry out cross-matching analysis across the whole electromagnetic spectrum. Here we considered several (i) low energy and multifrequency catalogs, listing sources detected in radio, infrared and optical surveys and or based on literature analyses,

and (ii) high energy catalogs, based on hard X-rays and γ -ray surveys.

It is worth noting that the 3PBC catalog is based on a moderate shallow survey thus we expect relatively bright sources in the hard X-rays to be also bright at lower energies, at least for the extragalactic population of 3PBC sources, being mainly constituted by AGNs. This limits the number of catalogs used to perform the cross-matching analysis and we used the same adopted in the original 3PBC analysis. Our analysis has been also augmented by using NED⁴ and SIMBAD⁵ databases, where we queried all sources having a low energy counterpart listed in the 3PBC before providing a final classification to verify the presence of updated literature information that is not reported in the catalogs adopted for the cross-matching analysis. All catalogs used in the current analysis are listed in Table 6.

2.1. Low energy catalogues for cross-matching analysis

At low frequencies, from radio to X-ray energies below 10 keV, we mainly considered:

1. The Revised Third Cambridge catalog⁶ (3CR, (Spinrad et al. 1985)). This catalog provides radio and optical data for 298 extragalactic sources, being the most powerful at low radio frequencies. It includes their positions, magnitudes, classification, and redshifts with only 25 sources being still unidentified (Massaro et al. 2013b; Maselli et al. 2016; Missaglia et al. 2021). More than 90% of the CR population have available multifrequency observations at radio, infrared, optical, and X-ray energies (see e.g. Massaro et al. 2015c; Maselli et al. 2016; Stuardi et al. 2018). The 3CR catalogue was create with a flux density limit $S_{178} \geq 2 \times 10^{-26} \text{ W m (Hz)}^{-1}$ at 178 MHz, spanning across the northern hemisphere with declination above -5 degrees. The 3CR catalog has been also augmented by a vast suite of multifrequency observations carried out in the last decades that provides all information necessary to have a completed overview of the source classification (Madrid et al. 2006; Privoon et al. 2008; Massaro et al. 2010, 2012c; Kotyla et al. 2016; Hilbert et al. 2016; Balmaverde et al. 2019; Jimenez-Gallardo et al. 2021; Balmaverde et al. 2021).
2. The Fourth Cambridge Survey catalog (4C)⁷ is based on the radio survey which used the large Cambridge interferometric telescope at the Mullard Radio Astronomy Observatory at frequency 178 Mc s^{-1} , detecting sources that have flux density $S_{178} \geq 2 \times 10^{-26} \text{ W m (Hz)}^{-1}$. It is published in two papers, the first one listing 1219 sources at declination between $+20^\circ$ and $+40^\circ$ (Pilkington & Scott 1965), while the second one includes 3624 sources in two declination ranges, -07° to $+20^\circ$ and $+40^\circ$ to $+80^\circ$ (Gower et al. 1967).
3. The Australia Telescope National Facility (ATNF)⁸ Pulsar catalog (Manchester et al. 2005) is a complete catalog listing more than 1500 pulsars (PSR). Accretion-powered X-ray PSRs are not included in this catalog, because they have different periods, unstable on short timescales. The catalog is based on the PSR database of 558 PSRs (Taylor et al. 1993) which was further supplemented by more recent PSR databases (Manchester et al. 2001; Edwards et al. 2001) to establish the ATNF PSR catalog.

⁴ <https://ned.ipac.caltech.edu/>

⁵ <http://simbad.cds.unistra.fr/simbad/>

⁶ <https://ned.ipac.caltech.edu/uri/NED::InRefcode/1985PASP...97..932S>

⁷ <http://astro.vaporia.com/start/fourc.html>

⁸ <https://heasarc.gsfc.nasa.gov/W3Browse/all/atnfpulsar.html>

4. The Catalog of Galactic Supernovae Remnants (SNRs) ⁹ (Green 2017), which is an updated version of the original catalog of galactic SNRs (Green 1984), currently listing 295 SNRs built on the available results published in literature updated to 2016.
 5. The 4th edition of the catalog of High mass X-ray binaries in the Galaxy ¹⁰ (Liu et al. 2006) provides 114 sources, updated with 35 new sources detected, most of them being X-ray binaries having a Be type star or a supergiant star as an optical companion.
 6. The 7th edition ¹¹ of the catalog of cataclysmic variables (CVs), low mass X-ray binaries and related objects (original paper Ritter & Kolb (2003)) lists 1166 cataclysmic variables, 105 low-mass X-ray binaries, and 500 related objects for a total of 1771 sources. The sources are provided with coordinates, apparent magnitudes, orbital parameters, stellar parameters, and other characteristics. The entire catalog is split into three tables provided online.
 7. The 4th edition of the catalog of Low mass X-ray binaries in the Galaxy and Magellanic Clouds¹² (Liu et al. 2007) contains 187 sources, updated by 44 newly discovered sources. The companion star of a Low mass X-ray binary is typically a K or M-type dwarf star. Small percentages of the companion stars are G type, red giants, or white dwarfs, and even smaller percentages of companions are A and F type stars. Sources are provided with their optical counterparts, spectra, X-ray luminosities, system parameters, stellar parameters of the components, and other parameters.
 8. The Catalog and Atlas of Cataclysmic Variables¹³ (CVcat, Downes et al. (2005)) presented its final release in January 2006 listing 1600 sources. The catalog provides all types of cataclysmic variables like novae, dwarf-novae, nova-like variables, sources classified only as CVs, interacting binary WDs, and possible supernovae. This catalog contains also all objects that have been classified as CVs at some point in the past and are no longer considered to be CVs. Those stars are labeled as NON-CV and are provided also with relevant references.
 9. To cross-match the sources with galaxy clusters we used only the Abell catalog of rich galaxy clusters¹⁴ (Abell et al. 1989). This catalog was conducted by a manual all-sky search for overdensities of galaxies on photographic plates. The catalog contains 4073 rich galaxy clusters, with at least 30 galaxies in magnitude range between m_3 and $m_3 + 2$, where m_3 is the magnitude of the third brightest cluster galaxy.
1. The 105 month *Swift*-BAT catalog¹⁵ (Oh et al. 2018) is created from data of a uniform hard X-ray all-sky survey in 14–195 keV band. It was developed using the same detector as the 3PBC catalog, but implementing different source algorithms to build X-ray images, data reduction, and source detection. Over 90 % of the sky is covered down to a flux limit of 8.40×10^{-12} erg cm⁻² s⁻¹ and over 50 % of the sky is covered down to a flux limit of 7.24×10^{-12} erg cm⁻² s⁻¹. The catalog provides 1632 hard X-ray sources detected above the 4.8σ level, presenting 422 new detections compared to the previous version of 70-month *Swift*-BAT catalog (Baumgartner et al. 2013). The catalog contains 1132 extragalactic sources, out of which 379 are Seyfert I and 448 Seyfert II type galaxies, 361 are Galactic sources and 139 are unidentified sources. Objects in the 105 month *Swift*-BAT catalogue are identified together with their optical counterparts by searching the NED and SIMBAD databases and archival X-ray data (e.g., *Swift*-XRT, *Chandra*, *ASCA*, *ROSAT*, *XMM-Newton*, and *NuSTAR*).
 2. The *INTEGRAL* IBIS survey hard X-ray catalogue¹⁶, (Bird et al. 2016)¹⁷ consists of 939 sources detected above a 4.5σ significance threshold in energy band 17–100, using the (IBIS) hard X-ray telescope (Winkler et al. 2003). The catalog showed 120 previously undiscovered soft γ -ray emitters. We also checked our results by comparing them to the findings in Krivonos et al. (2022).
 3. The second release of the fourth *Fermi*-LAT catalog of γ -ray sources¹⁸ (4FGL-DR2, Ballet et al. 2020), using the Large Area Telescope (LAT) on the *Fermi* Gamma-ray space telescope mission (Atwood et al. 2009), reports 723 new sources, increasing up to 5064 γ -ray sources. The catalog processed the first 10 years of the data in the energy range between 50 MeV to 1 TeV. The largest class of Galactic sources in the 4FGL-DR2 is constituted by PSRs listing 292 sources, while the extragalactic sample is dominated by blazars with 2226 identified and/or associated BL Lac objects and Flat spectrum radio quasars, and 1517 additional blazar candidates of uncertain type.

2.3. Multifrequency catalogs for low energy associations

1. The current 5th edition of Roma-BZCAT catalog of blazars based on multi-frequency surveys and extensive review of literature¹⁹ (Massaro et al. 2015a) lists coordinates and multifrequency data for 3561 sources which are either confirmed blazars or sources exhibiting blazar-like behavior. All sources included in the Roma-BZCAT are detected at radio frequencies. According to the Unified AGN model (Antonucci 1993; Urry & Padovani 1995), blazars are AGNs whose jet happens to be closely aligned with our line of sight, exhibiting strong variations, apparent superluminal motion, and emission extending across all electromagnetic spectrum.
2. The Turin-SyCAT (Peña-Herazo et al. 2022) multifrequency catalog of Seyfert galaxies was built using optical, infrared, and radio selection criteria. Seyfert galaxies are AGNs, which are distinguished as type 1 and type 2 based on the observer's angle (Antonucci & Miller 1985). All objects included in its 1st release have an optical spectroscopic classification, allowing us to establish precisely their redshifts

2.2. High energy surveys for cross-matching analysis

We also compared our classification of 3PBC sources with those of two hard X-ray catalogs (energies larger than 10 keV) and one of the latest releases of the Fermi catalog of γ -ray sources. The former comparison allows us also to obtain more information about the source classification in particular for the Galactic population, while the latter one allows us to look for any trend between the hard X-ray and the γ -ray emission for the class of blazars. To carry out this task we used the following catalogs.

⁹ <https://heasarc.gsfc.nasa.gov/W3Browse/all/snrgreen.html>

¹⁰ <https://heasarc.gsfc.nasa.gov/w3browse/all/hmxbeat.html>

¹¹ <https://heasarc.gsfc.nasa.gov/W3Browse/all/ritterlmxb.html>

¹² <https://heasarc.gsfc.nasa.gov/W3Browse/all/lmxbcat.html>

¹³ <https://heasarc.gsfc.nasa.gov/W3Browse/all/cvcat.html>

¹⁴ <https://heasarc.gsfc.nasa.gov/W3Browse/all/abell.html>

¹⁵ <https://heasarc.gsfc.nasa.gov/W3Browse/swift/swbat105m.html>

¹⁶ <https://heasarc.gsfc.nasa.gov/W3Browse/all/ibiscat.html>

¹⁷ <https://heasarc.gsfc.nasa.gov/W3Browse/integral/intibisass.html>

¹⁸ <https://heasarc.gsfc.nasa.gov/W3Browse/fermi/fermilpsc.html>

¹⁹ <http://www.ssdsc.asi.it/bzcat>

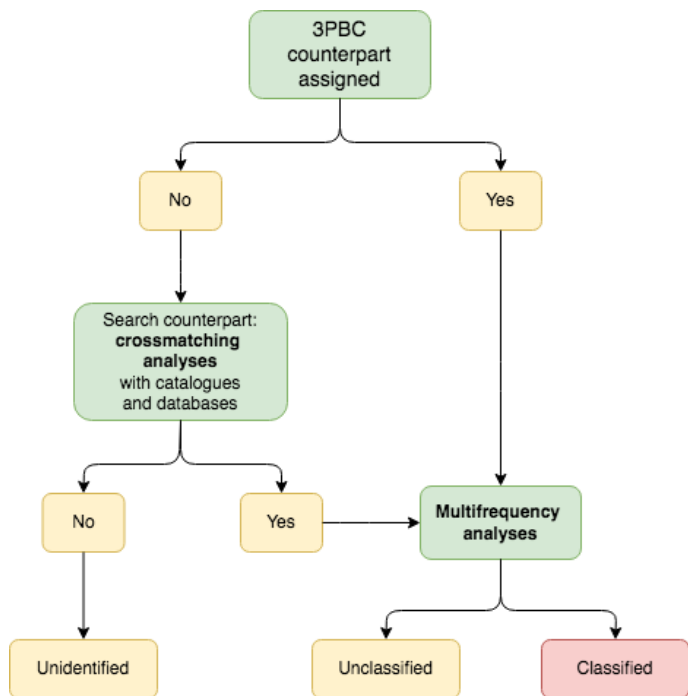


Fig. 1. The decision tree adopted in our analysis to distinguish between classified, unclassified, and unidentified hard X-ray sources (see Section 3.1 for a complete description).

and class. The catalog presents 351 Seyfert galaxies, out of which 233 are type 1 and 118 are type 2. In the analysis presented here, the 2nd release of the Turin-SyCAT, increased their number substantially by 80% to 633 Seyfert galaxies. Details can be found in Section 5. All Turin-SyCAT sources with a 3PBC counterpart are detected in the 3PBC at a signal-to-noise ratio above 6.

3. Classification

For classifying the sources considered in the presented analysis, we adopted the following step-by-step analysis, as shown in Figure 1 and according to the criteria outlined below. It is worth noting that we are not associating 3PBC sources with their low energy counterparts, but we only update the classification of the associated counterpart based on the latest release of several multifrequency catalogs as those previously listed, and/or follow-up observations that were performed after the 3PBC release (see e.g., Molina et al. 2009; Malizia et al. 2010, 2016; Landi et al. 2017; Ricci et al. 2017; Koss et al. 2017, and references therein).

3.1. Classification scheme

We start inspecting the 3PBC (Cusumano et al. 2010) catalogue. If a 3PBC source has an assigned counterpart we just adopted the multifrequency criteria reported below in this section to classify it. Then, for sources belonging to the extragalactic population, we also verified its redshift estimate. In particular, for all extragalactic sources, being the main focus of the current analysis, the presence of the optical spectrum or a description of it published in the literature is mandatory to consider it as *classified*.

For all sources lacking an assigned low energy counterpart in the original 3PBC, thus being unassociated, we perform the cross-matching analysis with all catalogs reported in section 2 and we also checked updated information in NED and SIMBAD

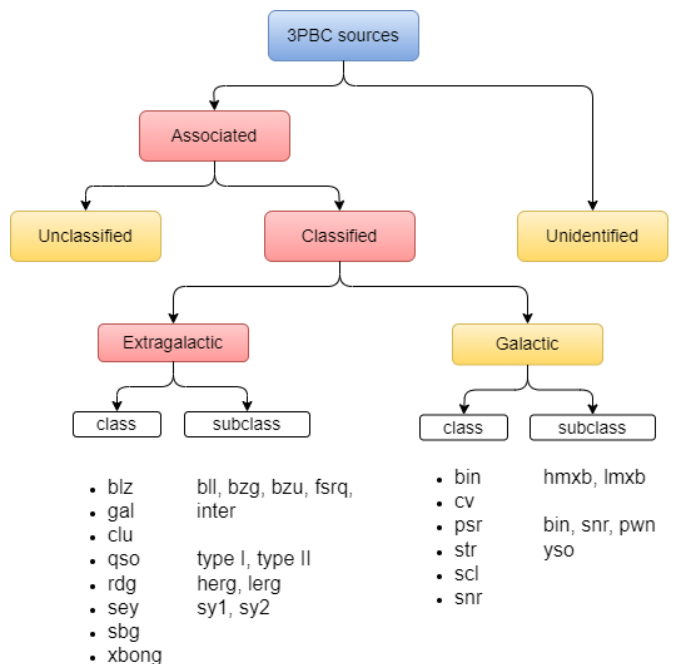


Fig. 2. Flowchart of the classification classes. Red cells represent categories leading to extragalactic sources, yellow are categories ending in non-extragalactic sources. Details about the numbers of sources in each class and subclass are described in Table 2 and Table 3. Note that classes and subclasses with only a few members are not included for clarity reasons.

databases, if any. If no reliable counterpart is found within the BAT positional uncertainty region, we flagged the 3PBC source as *unidentified*. On the other hand, if a potential counterpart is found, as in the previous step, we adopted the multifrequency criteria to classify it and eventually provide a redshift estimate, and, when successful, the associated source is indicated as *classified*.

Moreover, all associated sources that do not have optical spectrum available for their low energy counterpart and/or lack relevant information to determine their classification were labeled as *unclassified*.

All classified sources were then split into two main samples distinguishing between Galactic and extragalactic populations. The sky distribution for both the Galactic and the extragalactic populations are shown in Figure 2 and compared in Figure 5. We identified 9 classes and a few sub-classes for both the extragalactic and the Galactic sources discussed in detail in the following subsections, see Table 2 and Table 3.

3.2. Criteria, classes & distributions

3.2.1. Extragalactic sources

The largest fraction of sources identified in the extragalactic hard X-ray sky belongs mainly to the two classes of Seyfert galaxies and blazars (Oh et al. (2018), Paliya et al. (2019), Ajello et al. (2009)), of which the latter account for 10% - 20% of the entire survey population (Diana et al. 2022). Thus, given the possibility to use both the Roma-BZCAT and the Turin-SyCAT (Peña-Herazo et al. 2022), built on the basis of multifrequency criteria, for all 3PBC classified sources that belong to these two catalogs we adopted the same classification reported therein. Moreover,

we also used their classification schemes to identify new blazars and Seyfert galaxies, to help future releases.

Blazars (class symbol: *blz*) are the largest known population of γ -ray sources (Abdo et al. 2010a; Massaro et al. 2012a; Abdollahi et al. 2020), dominated by non-thermal radiation over the whole electromagnetic spectrum (Urry & Padovani 1995; Massaro et al. 2009). Their observational features also include high and variable polarization, superluminal motions, very high observed luminosities coupled with a flat radio spectrum (Healey et al. 2007; Hovatta et al. 2012) peculiar infrared colors (Massaro et al. 2011; D’Abrusco et al. 2012; Massaro et al. 2013c, 2014) and a rapid variability from the radio to X-ray bands with weak or absent emission lines (Stickel et al. 1991). Blandford & Rees (1978) suggested that radiation of blazars could be interpreted as arising from a relativistic jet closely aligned with the line of sight. Blazars were thus classified into 4 categories: BL Lac objects (subclass symbol: *bll*), with featureless optical spectra or presenting only relatively weak and narrow emission lines mainly due to their host galaxies. BL Lacs with their optical-UV spectral energy distribution dominated by the emission of their host galaxy has a subclass symbol: *bzg*. Flat spectrum radio quasars (subclass symbol: *fsrq*) show typical broad emission lines over a blue continuum. Sources exhibiting blazar-like broad-band features, but lacking optical spectroscopic classification are classified as blazars of uncertain type (subclass symbol: *bzu*). According to the nomenclature of the Roma-BZCAT BL Lacs and FSRQs are labeled as BZBs and BZQs, respectively, while, to avoid confusion here they are marked with the classification symbols *bll* and *fsrq*. This choice was adopted because, given the recent optical spectroscopic campaigns devoted to the search for γ -ray blazars (Landoni et al. 2015; Massaro et al. 2014; Ricci et al. 2015; Peña-Herazo et al. 2017; Paiano et al. 2017; Peña-Herazo et al. 2019; Paiano et al. 2020) a few more blazars, not yet listed in the Roma-BZCAT, were found as low energy counterparts of 3PBC sources and thus, to avoid confusion, we did not use the Roma-BZCAT nomenclature. No further BZGs and/or BZUs were discovered in our analysis and thus no different classification symbols with respect to those of the Roma-BZCAT were used in these cases.

Names for blazar-like counterparts of 3PBC sources were collected from the Roma-BZCAT if the source is listed therein otherwise in the final table the name reported in one of the major radio surveys as NVSS (Condon et al. 1998) and/or SUMSS (Bock et al. 1999; Mauch et al. 2003), taken from the NED database.

Seyfert galaxies (class symbol: *sey*) were originally defined mainly by their morphology (Seyfert 1943) as galaxies with high surface brightness nuclei. Nowadays, they are identified spectroscopically as (mostly spiral) galaxies with strong, highly ionized emission lines. Seyfert galaxies come in two flavors distinguished by the presence (or absence) of broad lines emission in their optical spectra (Khachikian & Weedman 1971, 1974). Type 1 Seyfert galaxies (subclass symbol: *sy1*) have both narrow and broad emission lines superimposed to their optical continuum. The former lines originate from a low-density ionized gas with density ranging between $\sim 10^3$ and 10^6 cm^{-3} and line widths corresponding to velocities of several hundred kilometers per second (e.g. (Vaona et al. 2012)), while broad lines are located only in permitted transitions, correspondent to electron densities of $\sim 10^9$ cm^{-3} and velocities of 10^4 km s^{-1} (e.g. Kollatschny & Zetzl (2013)). Type 2 Seyfert galaxies (subclass symbol: *sy2*) show only narrow lines in their optical spectra (e.g. Weedman 1977; Miyaji et al. 1992; Capetti et al. 1999).

To classify Seyfert galaxies we adopted all the same criteria reported in the Turin-SyCAT (Peña-Herazo et al. 2022) in terms of (i) presence of the optical spectrum in the literature, (ii) radio, infrared and optical luminosities, (iii) radio morphology. This was chosen because we include the new Seyfert galaxies discovered here in the 2nd release of the Turin-SyCAT as described in the following sections.

Names for Seyfert-like counterparts of 3PBC sources were collected from the 1st edition of the Turin-SyCAT if the source is listed therein otherwise, are reported in the main table with a NED name taken mainly out of one of the following catalogs: 1RXS (Voges et al. 1999), 2MASSS (Skrutskie et al. 2006), 2MASX (Jarrett et al. 2000) and BAT105 (Oh et al. 2018). All Seyfert galaxies were then renamed according to the Turin-SyCAT nomenclature.

All extragalactic sources that did not fall into the blazar and Seyfert classes mainly belong to the other two major classes: quasars and radio galaxies.

Quasars (QSOs), (class symbol: *qso*) are AGNs with bolometric luminosities above $\sim 10^{40}$ erg s^{-1} . They have broad spectral energy distribution and are emitting from radio up to hard X-ray energies, having variable flux densities almost at all frequencies, mid-IR emission due to the dusty torus, and broad emission lines superimposed to an optical blue continuum Schmidt (1969). For this extragalactic source class, we also distinguished type 1 and type 2 QSOs on the basis of the presence of broad emission lines in their optical spectra according to the same criteria adopted for the Seyfert galaxies (Khachikian & Weedman 1974). Then to distinguish a Seyfert galaxy from a QSO we also considered the same thresholds used to create the Turin-SyCAT (Peña-Herazo et al. 2022), indicating QSOs as sources with both (i) radio luminosity above 10^{40} erg s^{-1} and (ii) mid-IR luminosity estimate at $3.4\mu\text{m}$ above $10^{11}L_{\odot}$. Names for the QSOs counterparts of 3PBC sources were collected from is reported in the final table 4 with a NED name taken mainly from the following catalogues: 1RXS (Voges et al. 1999), 2MASSS (Skrutskie et al. 2006), 2MASX (Jarrett et al. 2000) and 1SXPS (Evans et al. 2014).

Radio galaxies (RDGs), (class symbol: *rdg*) are radio-loud AGNs whose radio emission is at least 100 times that of normal elliptical galaxies and extends beyond tens of kpc scale (Urry & Padovani 1995; Moffet 1966; Massaro et al. 2011; van Velzen et al. 2012), thus being neatly distinct from the Seyfert galaxies. On the other hand, to distinguish between QSO and RDG we adopted a radio morphological criterion where the latter clearly presents diffuse radio emission at a large scale when radio maps are available to check it. We used the same criteria and classification scheme recently adopted by (Capetti et al. 2017a,b). If the source was not listed with those names, we took the NED name mainly from 3C (Spinrad et al. 1985), 4C (Pilkington & Scott 1965; Gower et al. 1967) or 7C (Hales et al. 2007) catalogs.

We firstly classified RDGs on the basis of their radio morphologies at 1.4 GHz distinguishing between classical FR I and FR II sources (Fanaroff & Riley 1974). On the other hand, we also considered the two subclasses of radio galaxies defined on the basis of their optical emission lines, distinguishing between high excitation radio galaxies (HERGs), (subclass symbol: *herg*) and low excitation radio galaxies (LERGs), (subclass symbol: *lerg*) (Hine & Longair 1979). HERGs are almost always FRIIs, while LERGs can be either FRIs or FRIIs (Buttiglione et al. 2010).

We also considered galaxy clusters (class symbol: *clu*) as extragalactic sources of hard X-rays. Galaxy clusters are the largest gravity-bounded structures in the Universe, composed primarily

of dark matter, highly ionized and extremely hot intra-cluster gas of low density, and galaxies (Sarazin 1986; Giodini et al. 2009). Their X-ray emission is mainly due to bremsstrahlung radiation of relatively hot particles in their intra-cluster medium in the soft X-rays (i.e., between 0.5 and 10 keV Nevalainen et al. 2003), although a tail of this emission is also detectable at higher energies (Ajello et al. 2010). Since it is well known that some galaxy clusters were also detected by the BAT instrument on board SWIFT (Ajello et al. 2010) we reported 3PBC sources associated with them mainly when the cross-match with the Abell catalog indicated the possible presence of a galaxy cluster within the hard X-ray positional uncertainty region.

Finally, we highlight that a handful of extragalactic sources, not belonging to the five major classes listed above, fall into the following categories, being classified as starburst galaxies (class symbol: *sbg*), (Searle et al. 1973; Weedman et al. 1981), galaxies forming stars at unusually fast rates (10^3 times faster than in an average galaxy), X-ray bright optically normal galaxies (class symbol: *xbong*), which are normal galaxies, not hosting an AGN, but having substantial X-ray luminosity (Elvis et al. 1981; Comastri et al. 2002; Yuan & Narayan 2004), low-ionization nuclear emission-line region galaxies (class symbol: *liner*) (Singh et al. 2013) and normal galaxies (class symbol: *gal*), the latter not hosting an AGN but in a few cases interacting with nearby companions. Names of the 3PBC counterparts for those sources were collected mainly from 2MASX (Jarrett et al. 2000) and 2MASS (Skrutskie et al. 2006) catalogues.

We list a preview of the first 10 sources included in Table 4, our revised version of the 3PBC catalog in which we provide the 3PBC catalog name, coordinates, counterpart name, counterpart coordinates, spectroscopic redshifts, the classification in our class and subclass system and the WISE counterpart name. We show examples of spectra of a few objects in Figure 3 and Figure 4.

Table 2. Numbers of 3PBC extragalactic sources associated in each class and subclass.

Class symbol	Class number	Subclass symbol	Subclass number
blz	129	bll	30
		bzg	7
		bzu	24
		fsrq	68
gal	10	interacting	3
		-	7
clu	27		
liner	1		
qso	26	type 1	18
		type 2	1
		?	7
rdg	25	herg	21
		lerg	3
		?	1
sey	593	sy1	325
		sy2	268
sbg	5		
xbong	4		

Note: This is the classification of the 3PBC Galactic sources according to our classification scheme.

3.2.2. Galactic sources

In our Milky Way, most of the sources emitting in the hard X-rays are X-ray binaries (Grimm et al. 2002), while the second dominant class of hard X-ray sources is the cataclysmic variables (Revnivtsev et al. 2008).

X-ray binaries (BINs) (class symbol: *bin*) are systems of double stars containing compact stellar remnants, such as neutron stars, pulsars, or black holes, and a normal star which can range a variety of masses (e.g. Charles & Coe (2003); Knigge et al. (2011)). The compact stellar remnant accretes material from its companion, creating continual or transient X-ray emissions. X-ray binaries are classified based on their companion star distinguishing between low mass X-ray binaries (subclass symbol: *lmbx*) having the companion star of mass $\lesssim 1 M_{\odot}$ and high mass X-ray binaries (subclass symbol: *hmbx*) usually accompanied by a star of mass $\gtrsim 10 M_{\odot}$, where the accretion happens directly from a stellar wind of the companion star. Names for the BINs counterparts of 3PBC sources were collected mainly from the following catalogues: IGR (Bird et al. 2004), 1H, SWIFT (Ajello et al. 2010) and (RX+XTE+SAX) (Bade et al. 1992; Voges et al. 1999; Frontera et al. 2009).

Cataclysmic variables (CVs), (class symbol: *cv*) are binary systems composed of a main-sequence companion star and a compact stellar remnant which is a white dwarf (WD) (Revnivtsev et al. 2008). The accretion happens almost always via filling the Roche-lobe of the companion star and subsequent formation of an accretion disk around the WD (Warner 1995). Their X-ray emission can originate from a variety of processes depending on the type of the CV. CVs which do not have strong magnetic fields accrete matter closer to the surface of the WD and produce sporadic eruptions. For 4 sources belonging to the CV class, we also indicated if they are symbiotic stars or novae, however, given their relatively low number with respect to all CVs identified we did not label these as subclasses and we only report the source class. Names for the CVs counterparts of 3PBC sources were collected mainly from the following catalogues: CV (Downes et al. 2005), IGR (Bird et al. 2004), 1RXS (Voges et al. 1999) and 2MASS (Skrutskie et al. 2006).

The hard X-ray sky is also populated by isolated X-ray pulsars (PSR), (class symbol: *psr*), not being hosted in X-ray binaries. Since they can be indeed hosted in pulsar wind nebulae (subclass symbol: *pwne*) or supernova remnants we highlight the presence of this extended emission around the PSR in the subclass column. On the other hand, if the hard X-ray emission is indeed due to a supernova remnant not hosting a neutron star then we adopted a different class (subclass symbol: *snr*), in these cases, their hard X-ray emission is due to the thermal radiation of plasma heated in shocks, coupled with non-thermal synchrotron radiation (see e.g., Vink (2012)). Names for the PSRs counterparts of 3PBC sources were collected mainly from the ATNF PSR catalog or other radio surveys.

As occurred for the extragalactic hard X-ray population a handful of sources were also identified belonging to normal stars (class symbol: *str*), (coming with a subclass: *ysc* for young stellar objects) and star clusters (class symbol: *sc*). X-ray emission from main sequence stars of masses $> 10 M_{\odot}$ can be due to discrete ionized metal lines in their spectrum. Young stellar objects, protostars, and T Tauri stars also exhibit X-ray radiation, predominantly emerging from magnetic coronae accreting material where shocks occur (Güdel & Nazé 2009). On the other hand, star clusters can appear as an amalgamation of point-like sources and extended X-ray emissions. Their point-like component can be produced by hot stars and/or SNR, lasting a few

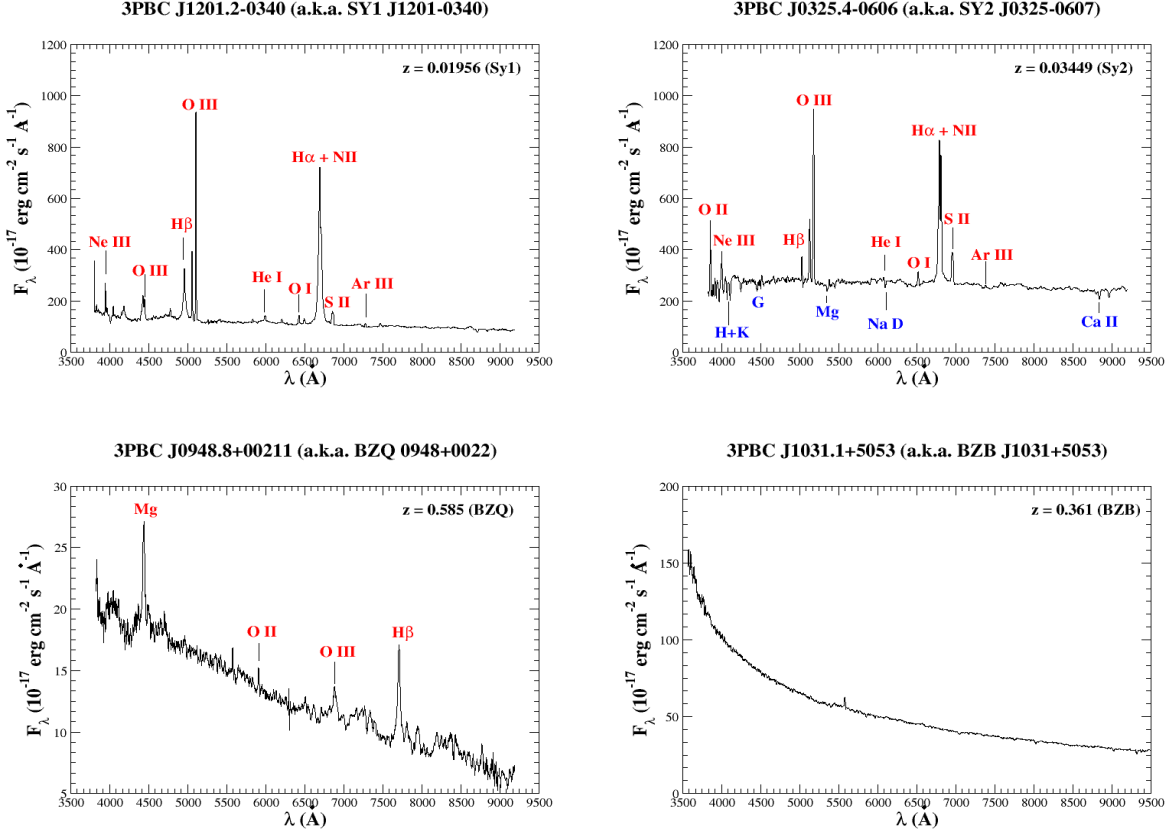


Fig. 3. Four images showing examples of the optical spectra of 3PBC counterparts identified in our refined analysis. Top left: Type I Seyfert galaxy 3PBCJ1201.2-0340. Top right: Type II Seyfert galaxy 3PBCJ0325.4-0606. Middle left: Flat spectrum radio quasar (fsrq) 3PBCJ0948.8+0021. Middle right: BL Lac object 3PBCJ1031.1+5053 (BZB in Roma-BZCAT (Massaro et al. 2009) nomenclature).

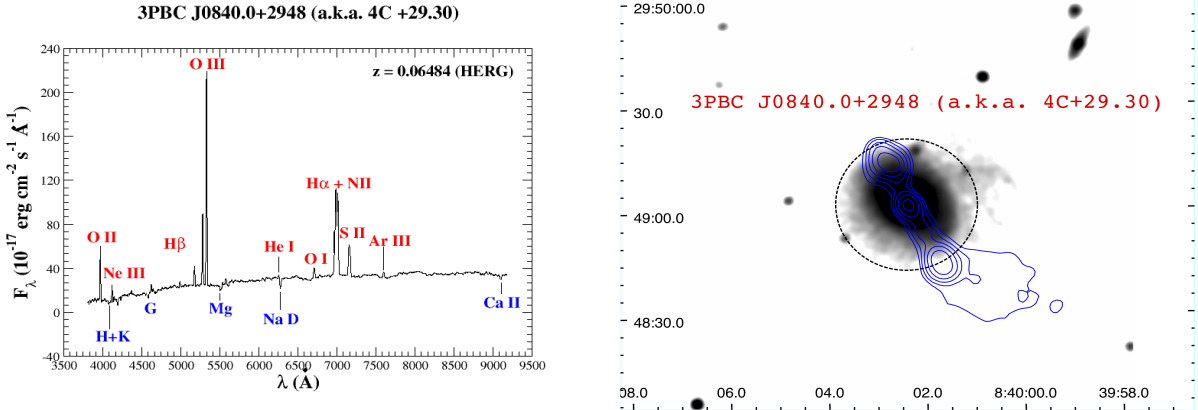


Fig. 4. Left panel: the optical spectrum of the HERG 4C +29.30 associated with 3PBCJ0840.0+2948 where main spectral emission and/or absorption lines are marked. Right panel: the optical image from the Pan-STARRS archive in the r band of 4C +29.30 with radio contours overlaid, drawn from the 3 GHz VLASS²⁰ radio map extending beyond the host galaxy.

thousand years while their extended component is produced by star cluster wind, formed by the interaction of stellar winds of massive O or B type stars, Wolf-Rayet stars, and supernovae explosions (e.g. Cantó et al. (2000); Law & Yusef-Zadeh (2004); Oskinova (2005)). In addition to them we also reported the classification for one microquasar (class symbol: *mqso*), namely: 3PBC J0804.7-2748. Microquasars are similar to quasars but

in a much smaller case. Their radiation comes from a stellar mass black hole or a neutron star accreting matter from a normal star (Mirabel 2010). In addition, we report one planetary nebula (class symbol: *pn*): 3PBC J1701.5-4306. Planetary nebulae are the ejected red giant's atmosphere ionized by the leftover star's core, forming at the end of life of stars with initial masses in the

range ~ 1 to 8 solar masses. Lastly, we also labeled the Galactic center Sgr A* with the symbol: *galcent*.

Table 3. Numbers of the Galactic 3PBC sources associated in each class and subclass.

Class symbol	Class number	Subclass symbol	Subclass number
bin	231	hmx	117
		lmx	108
		?	6
cv	83		
str	12	-	6
		ys	1
		?	1
psr	21	bin	1
		-	5
		snr	12
		pwn	3
scl	2		
snr	4		
mqso	1		
pn	1		
galcent	1		

Note: This is the classification of the 3PBC Galactic sources according to our classification scheme. Classes: *galcent*, *mqso*, and *pn* were omitted due to a small member count (1 each).

3.2.3. Sky distributions

Starting from the total number of 1593 sources listed in the 3PBC catalogue (Cusumano et al. 2010) we found that according to our analysis there are 218 unidentified hard X-ray sources ($\sim 13.7\%$) and 199 unclassified sources ($\sim 12.5\%$), see Figure 5. The classified sources are distinguished into two main groups: Galactic objects including 356 sources ($\sim 22.2\%$), and extragalactic objects having 820 sources ($\sim 51.5\%$).

We show the sky distribution of 3PBC sources via the Hammer-Aitoff projection for both unclassified and unidentified cases in Figure 6 and for classified sources, distinguishing between Galactic and extragalactic ones in Figure 7. Given the source distributions for both unidentified and unclassified sources that appear to be quite uniform over the whole sky, we could expect that a large fraction of them could have an extragalactic origin. This could imply that the lack of classified counterparts is mainly due to missing follow-up spectroscopic observations, thus strengthening the need to complete optical campaigns carried out to date (see e.g. Masetti et al. 2009; Cowperthwaite et al. 2013). Then fractions of other classes for extragalactic sources are shown in Figure 9 and for Galactic classes in Figure 8.

4. Characterizing the Extragalactic Hard X-Ray Sky

Our revised analysis of the 3PBC lists 820 extragalactic sources, classified into 9 classes: 129 blazars (*blz*), 10 galaxies (*gal*), 27 galaxy clusters (*clu*), 1 low-ionization nuclear emission-line region galaxy (*liner*), 26 quasars (*qso*), 25 radio galaxies (*rdg*), 593 Seyfert galaxies (*sey*), 5 star-burst galaxies (*sbg*) and 1 X-ray bright optically normal galaxy (*xbong*). Table 2 reports those numbers together with the number of sources in their associated subclasses.

Table 4. Our revised version of the 3PBC catalog. The entire catalogue table is available in the online material.

3PBC name	R.A. ^{3PBC} (deg)	Dec. ^{3PBC} (deg)	counterpart name	R.A. ^{cp} (deg)	Dec. ^{cp} (deg)	z	class	subclass	WISE name
J0000.9-0708	0.228	-7.134	2MASS J00004877-0709115	0.203216	-7.153221	0.03748	sey	sy2	J000048.77-070911.6
J0001.7-7659	0.429	-76.986	2MASX J00014596-7657144	0.441917	-76.953972	0.05839	sey	sy1	J000146.08-765714.2
J0002.5+0322	0.636	3.367	SY1 J0002+0322	0.610046	3.351961	0.025518	sey	sy1	J000226.42+032106.8
J0002.5+0322	0.853	27.638	2MASX J00032742+2739173	0.864283	27.654828	0.03969	sey	sy2	J000327.41+273917.0
J0002.5+0322	1.009	70.312	SY2 J0004+7020	1.008228	70.32175	0.096	sey	sy2	J000401.97+701918.3
J0006.3+2012	1.584	20.205	SY1 J0006+2013	1.581389	20.202968	0.025785	sey	sy1	J000619.53+201210.6
J0010.4+1058	2.624	10.976	5BZQ J0010+1058	2.629166	10.974888	0.089100	blz	fsrq	J001031.00+105829.5
J0016.7-2611	4.194	-26.2		0.	0.	0.	uhx		
J0017.4+0519	4.37	5.326	HS 0014+0504	4.344167	5.352778	0.11	sey	sy1	J001722.71+052111.4
J0017.8+8135	4.454	81.591	5BZQ J0017+8135	4.28525	81.58561	3.387000	blz	fsrq	J001708.50+813508.1

Only the first 10 lines are reported here. Col. (1) 3PBC source name; Cols. (2,3) Right Ascension and Declination of the 3PBC source (Equinox J2000); Col. (4) name of the counterpart assigned in our refined analysis; col. (5,6) Right Ascension and Declination of the counterpart (Equinox J2000); Col. (7) counterpart redshift if extragalactic; Cols. (8,9) class and subclass assigned according to our classification scheme; Col. (10) WISE name of the counterpart.

The most abundant class of extragalactic sources are Seyfert galaxies (Figure 9), while the second largest population of extragalactic sources emitting in the hard X-rays is constituted by blazars. The hard X-ray luminosity, K-corrected, is shown in Figure 10 as a function of the redshift with particular emphasis on the two classes of Seyfert galaxies and blazars. We used the measured spectral index reported in the 3PBC for K-correlation computation.

Once we assigned the coordinates of each counterpart we also crossmatched the 3PBC catalog with the AllWISE survey²¹ (Cutri et al. 2021) and we found that adopting an association radius of $3.3''$, as typically used in other analyses (D'Abrusco et al. 2019; Massaro et al. 2012b; de Menezes et al. 2020) we found 1279 mid-IR counterparts in the 1593 3PBC sources. It is worth noting that associating sources within this angular separation corresponds to a chance probability of having a spurious match lower than $\sim 2\%$ (Massaro et al. 2013a, 2015b).

We also used the counterpart coordinates to carry out a cross-match between all blazars listed in the 3PBC and those associated with the 4FGL catalog. There are 92 out of 129 blazars with a *Fermi* counterpart and with known redshift, with 25 of them belonging to the BL Lac class and 52 to that of FSRQs. For all these γ -ray emitting blazars we also found two neat trends/correlations between their hard X-ray and γ -ray emissions as highlighted in Figure 11. The first trend is between their hard X-ray and γ -ray fluxes, where a mild correlation is also reported: 0.52 is the measured value for the correlation coefficient for the whole blazar sample. The p-chance for all correlations is below 10^{-5} level of significance due to the high number of sources used to compute the correlation coefficients. Then a second trend was indeed found between the photon indices of blazars measured in the 3PBC and in the 4FGL catalogs.

Both trends highlighted for the blazar population emitting in the hard X-rays are expected given the nature of their emission (e.g. Acharyya et al. (2021)). For BL Lac objects the steep hard

X-ray spectra could be due to emission arising from the tail of their synchrotron (Maraschi et al. 1992) component, and the flat γ -ray spectra are related to the peak of their inverse Compton bump at γ -ray energies (Maraschi et al. 1999; Marscher & Gear 1985; Dermer 1995). On the other hand for the FSRQs both the hard X-ray and the γ -ray emission are due to their inverse Compton component peaking in the γ -ray band (Acharyya et al. 2021). Then we also note that even if the broadband spectral energy distributions (SEDs) of BL Lacs are mainly interpreted as due to Synchrotron Self Compton emission while that of FSQRs to external Compton radiation (Abdo et al. 2010b) relativistic particles responsible for both SED bumps are the same and thus we could expect that fluxes in the hard X-rays and in the γ -rays are, on average, connected (Wolter et al. 2008, see e.g.).

5. Second Release of the Turin-SyCAT

We found 282 new Seyfert galaxies resulting from our analysis of the extragalactic hard X-ray sky presented in the previous sections. Adding all new Seyfert galaxies to those already included in the 1st release of the Turin-SyCAT its 2nd release lists 633 Seyfert galaxies: 351 types 1 and 282 types 2. Thus we added a total of 118 types 1 and 164 types 2 Seyfert galaxies and we also present here an updated analysis of the infrared - hard X-ray connection including all new sources.

Sources added in the 2nd release of the Turin-SyCAT were selected according to the same procedure as in Peña-Herazo et al. (2022). These strict selection criteria allow us to have a negligible fraction of contaminants since we selected only extragalactic sources with a Seyfert-like optical spectrum and having:

1. a published optical spectrum;
2. a luminosity in Radio lower than $<10^{40}$ erg s⁻¹ if a counterpart is listed in the two major radio surveys (i.e., NVSS and SUMSS Condon et al. 1998; Mauch et al. 2003, respectively);
3. a counterpart in the AllWISE Source catalog with a mid-IR luminosity at $3.4\mu m$ less than $3 \times 10^{11} L_{\odot}$. This was mainly adopted to avoid the selection of QSOs.

In Figure 12 we present the redshift distribution of Turin-SyCAT 2nd release. The source number for both classes drastically drops after $z > 0.2$ as occurs for those listed in the first release, and the source with the highest redshift is SY2 J0304-3026 at 0.436. We compare the redshift distribution of all Seyfert galaxies (Figure 13), only Type 1 Seyfert galaxies (Figure 14) and only Type 2 Seyfert galaxies (Figure 15) between the 1st release of the Turin-SyCAT and its presented 2nd release.

With respect to the previous Turin-SyCAT 1st release, we modified the name of SY2 J2328+0330 in SY2 J2329+0331 having a WISE counterpart J232903.90+033159.9 and since a new Seyfert type 2 galaxy was associated with its mid-IR counterpart J232846.65+033041.1 thus being named as SY2 J2328+0330.

We list all sources included in the Turin-SyCAT 2nd release in Table 5 where we provide SyCAT 1st release and SyCAT 2nd release ids, SyCAT name, coordinates, spectroscopic redshifts, WISE counterpart, and 3PBC counterpart names, flux and flags to indicate if the source is also associated in 3PBC and BAT105 catalogs, and a flag to point out those added in this 2nd release.

On the basis of the new Seyfert galaxies discovered here, we refined the connection between their hard X-ray and the mid-IR emission (Assef et al. 2013). This connection is related to

²¹ <https://wise2.ipac.caltech.edu/docs/release/allwise/>

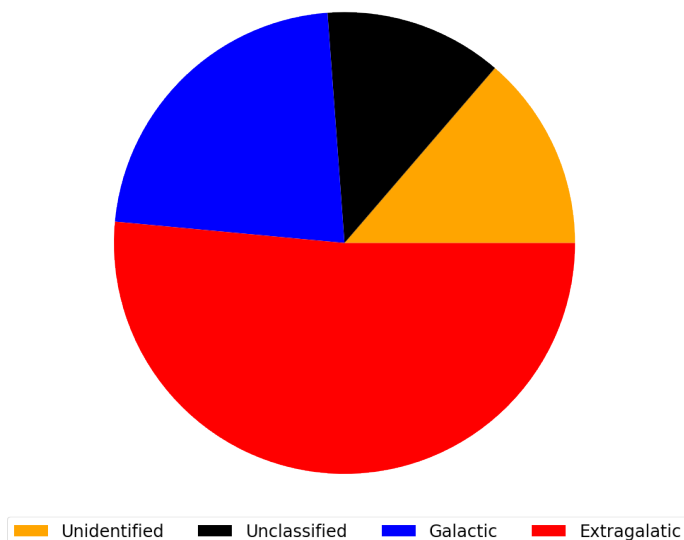


Fig. 5. Pie-chart showing the fractions of the main classification categories derived thanks to our revised analysis of the 3PBC. The representation of the categories is following: 218 Unidentified ($\sim 13.7\%$), 199 Unclassified ($\sim 12.5\%$), 356 Galactic ($\sim 22.3\%$), 820 Extragalactic ($\sim 51.5\%$).

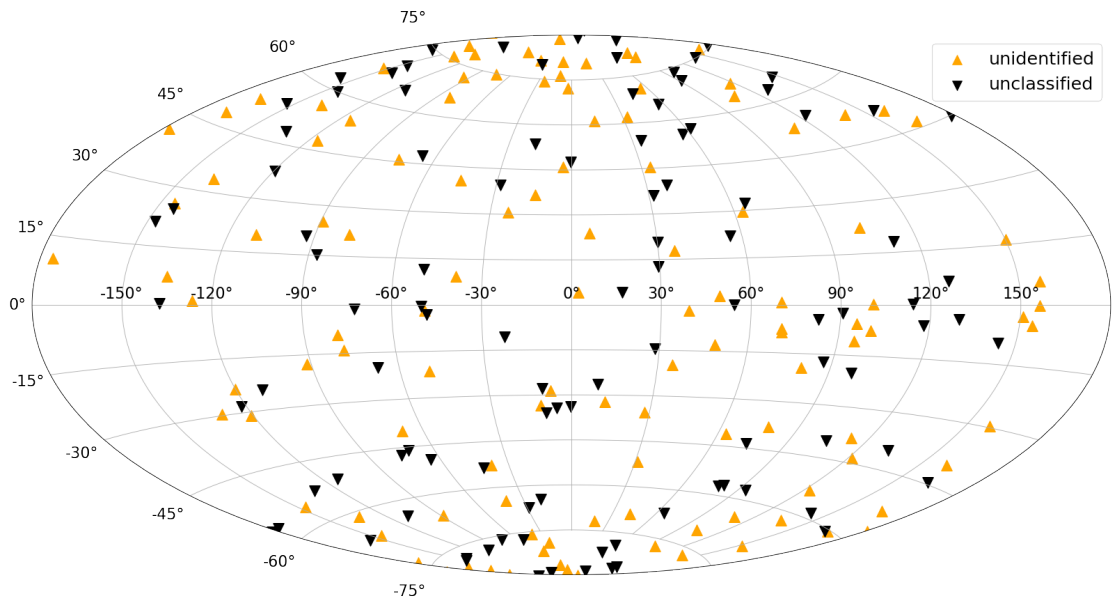


Fig. 6. Hammer-Aitoff projection derived thanks to our revised analysis of the 3PBC, showing unidentified and unclassified sources.

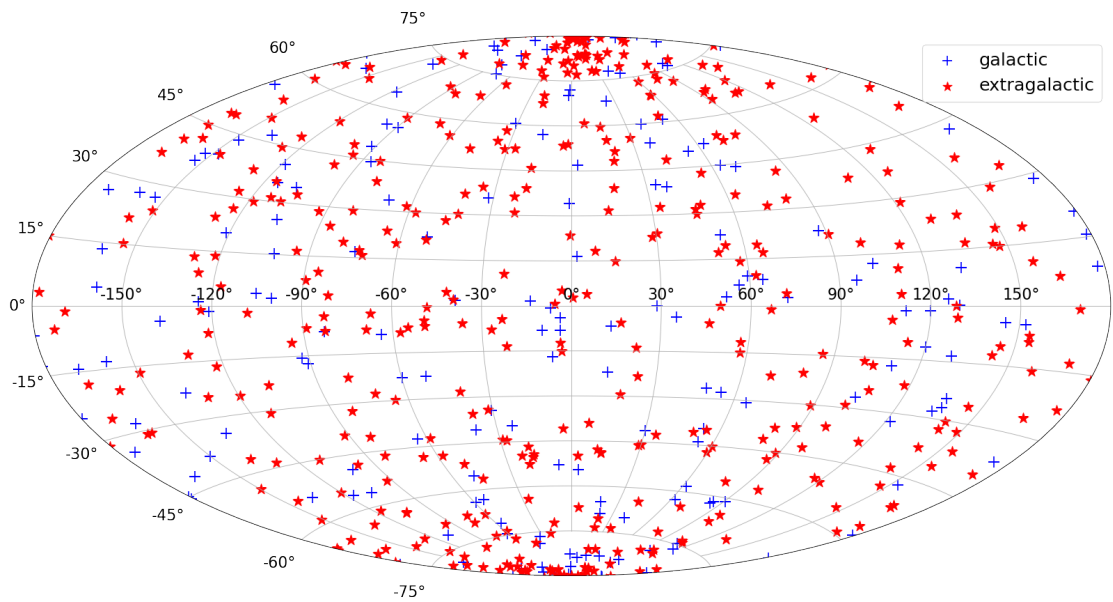


Fig. 7. Hammer-Aitoff projection based on our revised analysis of the 3PBC, showing Galactic and extragalactic sources.

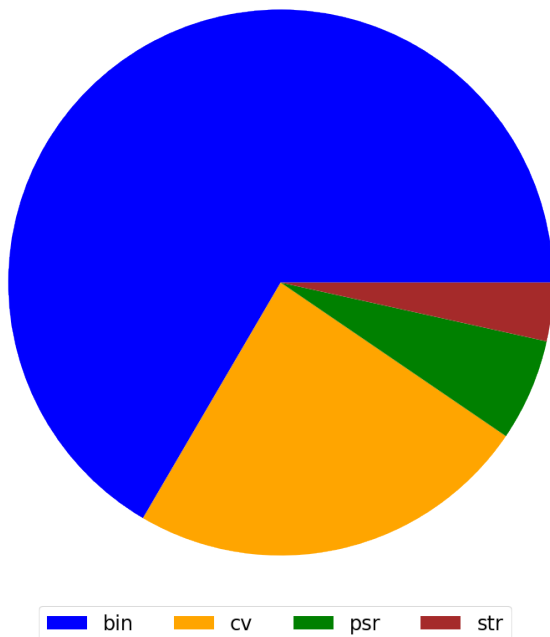


Fig. 8. Pie-chart showing the fractions of galactic classes derived thanks to our revised analysis of the 3PBC. The classes are represented as follows: 231 bin ($\sim 66.6\%$), 83 cv ($\sim 23.9\%$), 21 psr ($\sim 6.1\%$), 12 str ($\sim 3.5\%$). Note, that classes galcent, mqso and pn are omitted for a small contribution (1 member each).

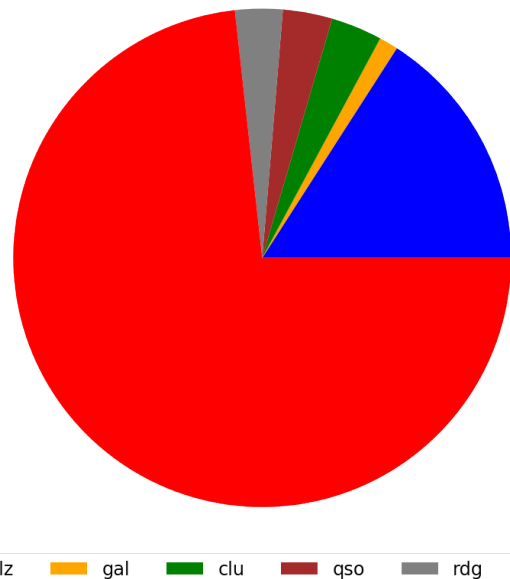


Fig. 9. Pie-chart showing the fractions of extragalactic classes derived thanks to our revised analysis of the 3PBC. Individual classes have following representation: 129 blz ($\sim 15.9\%$), gal 10 ($\sim 1.2\%$), 27 clu ($\sim 3.3\%$), 26 qso ($\sim 3.2\%$), 25 rdg ($\sim 3.1\%$), 593 sey ($\sim 73.2\%$). Note that the liner, xbong, and sbg subclasses are omitted for a small contribution (1, 4, and 5 members each, respectively).

the reprocessed radiation from the dust of all energy absorbed from the optical and UV wavelengths in the central engine of Seyfert galaxies (e.g. Elvis et al. (2009)). The high-energy emission measures an intrinsic radiated luminosity above ~ 10 keV, while WISE $12\ \mu\text{m}$ and $22\ \mu\text{m}$ is related to the reprocessed radiation from the dust of all energy absorbed from the optical and UV wavelengths.

Mid-IR fluxes show a significant correlation with the hard X-ray fluxes, similar to those highlighted using Seyfert galaxies listed in the Turin-SyCAT 1st release, as shown in Figure 16. Comparing integrated fluxes as F_{12} and F_{HX} we found a linear correlation coefficient of 0.54 (correspondent to a slope of 1.09 ± 0.10 given the measured dispersion) for Seyfert 1 and 0.45 (slope of 1.20 ± 0.16) for Seyfert 2 galaxies, respectively. F_{12} is the integrated flux at 12 microns derived from the WISE magnitude and F_{HX} is the integrated hard X-ray flux in the 15-150 keV energy range both in units of $\text{erg cm}^{-2} \text{s}^{-1}$. This is in agreement with results presented on the statistical analysis of Seyfert galaxies listed in the Turin-SyCAT 1st release where we measured a correlation coefficient of 0.57, with a slope of 1.02 ± 0.10 and a coefficient of 0.52 (slope of 0.93 ± 0.16), for Seyfert 1 and 2 galaxies, respectively. On the other hand, also comparing mid-IR at lower frequencies with the hard X-ray flux (i.e., F_{22} vs F_{HX}), where F_{22} is the integrated flux at 22 microns derived from the WISE magnitude in units of $\text{erg cm}^{-2} \text{s}^{-1}$, we found a correlation coefficient of 0.55 (with a slope of 1.11 ± 0.10) for type 1 Seyfert galaxies and 0.46 (slope of 1.08 ± 0.17) for type 2 Seyfert galaxies.

Considering both classes together, since they show similar mid-IR to hard X-ray ratios, we found a correlation coefficient of 0.51 and a slope of 1.1 ± 0.08 for both hard X-ray flux F_{HX} correlation with F_{12} and F_{22} , all in agreement with previous results based on the Turin-SyCAT 1st release.

Hard X-ray luminosities

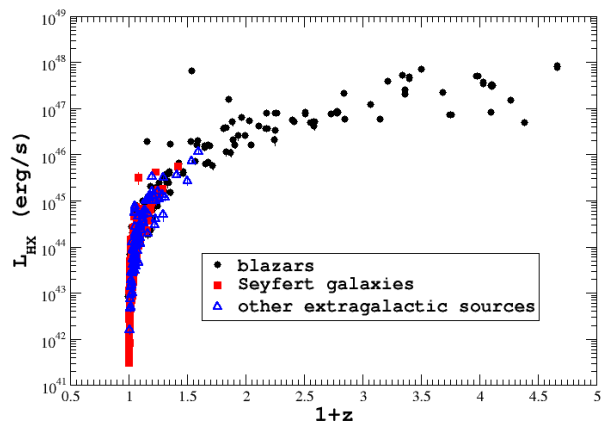


Fig. 10. K-corrected hard X-ray luminosity computed using the 15-150 keV flux reported in the 3PBC. Given the high numbers of sources used to compute the correlation coefficients, the p-chance for all correlations is below 10^{-5} level of significance. Seyfert galaxies are reported as red squares, blazars as blue circles while all other extragalactic sources are marked as green triangles. Statistical uncertainties are smaller than the size of the points.

We also cross-matched sources listed in Turin-SyCAT 2nd release with the Point Source catalog of the Infrared Astronomical Satellite (*IRAS*)²², using the positional uncertainties reported therein. We obtained 67 new matches for a total of 216 Seyfert galaxies with an IRAS counterpart, 89 types 1 and 127 types 2 counterparts at both $60\ \mu\text{m}$ and $100\ \mu\text{m}$, respectively. Then,

²² <https://heasarc.gsfc.nasa.gov/W3Browse/iras/iraspsc.html>

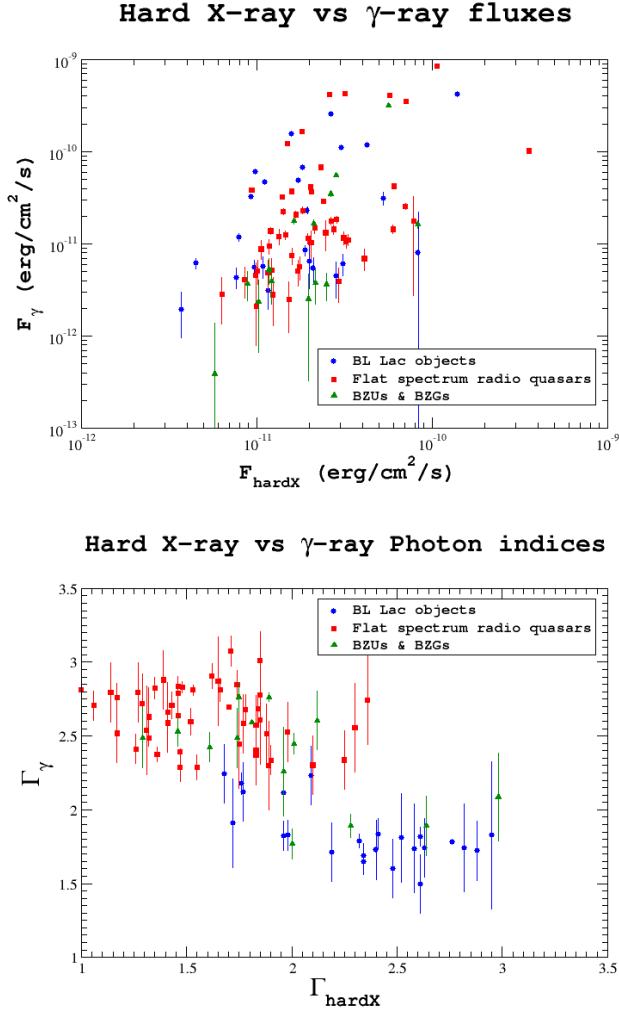


Fig. 11. Top: Hard X-ray vs γ -ray and vs photon indices (bottom) correlation of all blazars in our sample. We can see, that BL Lacs are steeper in hard X-rays and flatter in γ -rays (bottom), however, their Hard X-ray vs γ -ray flux distribution (top) appears similar.

as occurred in our previous analysis (Peña-Herazo et al. 2022), we also tested possible trends between the infrared fluxes, at $60 \mu\text{m}$ and at $100 \mu\text{m}$, and the hard X-ray one. We found no clear correlation as evident in Figure 17 and again these results are in agreement with our previous findings based on Turin-SyCAT 1st release. Moreover, we did not expect any correlation while inspecting trends between infrared and hard X-ray fluxes since the cold dust, mainly responsible for the emission at $60 \mu\text{m}$ and $100 \mu\text{m}$ is not significantly affected by the behavior of the central AGN but it is mainly linked to the star formation occurring in Seyfert galaxies (Rodríguez Espinosa et al. 1987).

The strict multi-frequency selection criteria that we used to select Turin-SyCAT sources allowed us to minimize the possible contamination of other source classes, thus strengthening our results. Thus we remind that we visually inspected all Turin-SyCAT galaxies’ optical spectra, allowing us to measure their redshifts and establish their proper optical classification.

Table 5. The 2nd version of the Turin-SyCAT catalog. Only the first 10 rows, the full catalog table is available in the online material.

IDv2 (1)	IDv1 (2)	SyCAT (3)	R.A. (4)	Dec. (5)	z (6)	WISE (7)	3PBC (8)	F_{HX} (9)	3PBC flag (10)	BAT105 flag (11)	SyCAT v2 flag (12)
1		SY2 J0000-0709	0.203216	-7.153221	0.03748	J000048.77-070911.6	3PBC J0000.9-0708	1.25E-11 \pm 1.4E-12	✓	✓	✓
2		SY1 J0001-7657	0.441917	-76.953972	0.05839	J000146.08-765714.2	3PBC J0001.7-7659	1.09-11 \pm 1.5E-12	✓	✓	✓
3	1	SY1 J0002+0322	0.6102917	3.352	0.025518	J000226.41+032107.0	3PBC J0002.5+0322	1.39E-11 \pm 1.9E-12	✓	✓	–
4		SY2 J0003+2739	0.864283	27.654828	0.03969	J000327.41+273917.0	3PBC J0003.4+2738	1.82E-11 \pm 2.6E-12	✓	✓	–
5	2	SY2 J0004+7020	1.00817	70.32175	0.096	J000401.97+701918.2	3PBC J0004.0+7018	1.1E-11 \pm 1.30E-12	✓	✓	–
6	3	SY1 J0006+2013	1.58133	20.202917	0.025785	J000619.53+201210.6	3PBC J0006.3+2012	1.76E-11 \pm 1.40E-12	✓	✓	–
7		SY1 J0017+0521	4.344167	5.352778	0.11	J001722.71+052111.4	3PBC J0017.4+0519	8.69E-12 \pm 1.5E-12	✓	✓	✓
8		SY2 J0021-1910	5.281417	-19.168222	0.09558	J002107.53-191005.4	3PBC J0021.1-1909	1.76E-11 \pm 1.60E-12	✓	✓	✓
9	4	SY2 J0025+6821	6.38542	68.3622	0.012	J002532.37+682144.9	3PBC J0025.5+6822	1.79E-11 \pm 1.40E-12	✓	✓	–
10	5	SY1 J0025-1859	6.4265	-19.002917	0.24622	J002542.34-190010.1	3PBC J0025.6-1859	1.05E-11 \pm 1.60E-12	✓	–	–

Column description: (1) Unique catalog identified (ID) from SyCAT 2nd version; (2) Unique catalog identified (ID) from SyCAT 1st version; (3) SyCAT name; (4) Right Ascension J2000; (5) Declination J2000; (6) Redshift; (7) name in WISE; (8) name in 3PBC; (9) Flux; (10) flag if the source is in 3PBC; (11) flag if the source is in BAT105; (12) flag if the source was added in SyCAT v2.

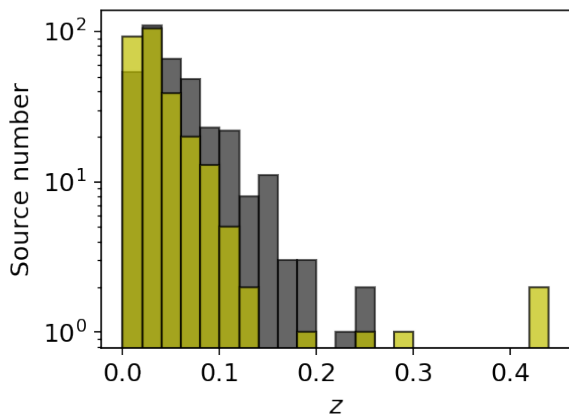


Fig. 12. Redshift distribution of Turin-SyCAT Seyfert galaxies. Type 1 in black, type 2 in yellow.

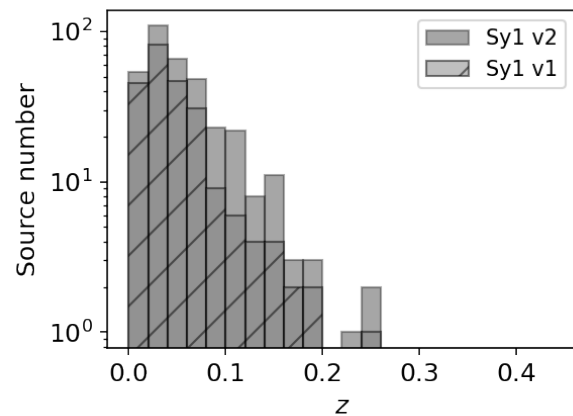


Fig. 14. Redshift distribution of Type 1 Seyfert galaxies from 1st release of the Turin-SyCAT compared to the presented 2nd release.

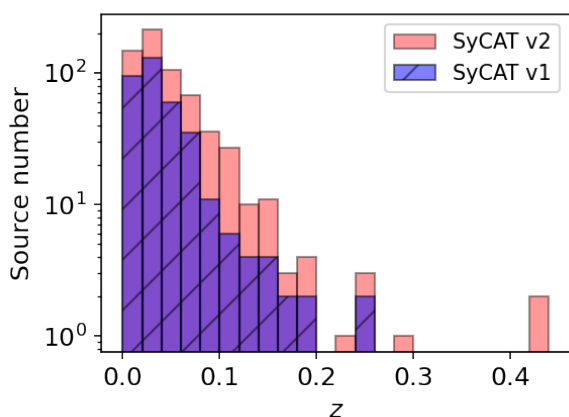


Fig. 13. Redshift distribution of all Seyfert galaxies from 1st release of the Turin-SyCAT compared to those listed in the 2nd release.

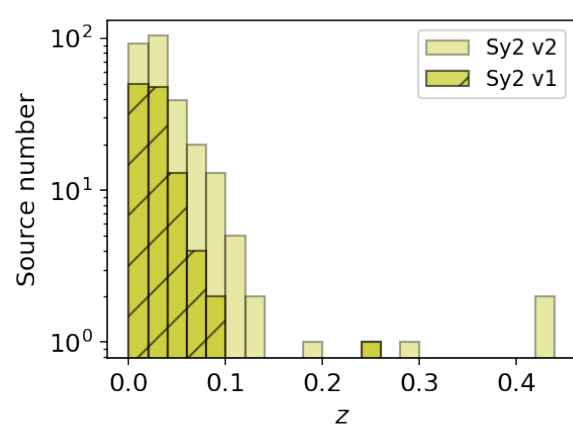


Fig. 15. Redshift distribution of Type 2 Seyfert galaxies from 1st release of the Turin-SyCAT compared to the presented 2nd release.

6. Summary, Conclusions and Future Perspectives

The CXB is nowadays established to constitute mainly an integrated emission of discrete sources, primarily arising from AGNs (Gilli et al. 2007). Having a precise knowledge of the population and properties of various types of AGNs is thus crucial to improving our knowledge of the CXB.

In this work, we focus on the analysis of the 3PBC catalog (Cusumano et al. 2010), in particular focusing on the extragalactic source population, aiming also at discovering new Seyfert galaxies that can be included in the presented Turin-SyCAT 2nd release. The 3PBC provides 1593 sources above signal to noise ratio of 3.8, approximately 57% sources appear to have a clear extragalactic origin while 19% belong to our Milky Way, and the remaining 24% are yet unknown. Results of our multifrequency investigation are also based on those recently found for the 105 month *Swift*-BAT catalogue (Oh et al. 2018) and the *INTEGRAL* IBIS hard X-ray survey in energy range 17-100 keV (Bird et al. 2016). For comparison, the original release of the 3PBC catalog listed 521 Seyfert galaxies, 109 blazars, 362 unclassified sources, and 244 unidentified sources, all classified according to our classification scheme while in the refined version presented here there are 593 Seyfert galaxies, 129 blazars, 199 unclassified sources, and 218 unidentified sources. It is worth highlighting

that, on the basis of our classification criteria, we indicated 98 sources as unclassified, even though they had an assigned class in the original 3PBC catalog, due to a lack of information. All details about how we interpreted 3PBC original classes according to our classification scheme are reported in Appendix A and Table A.1.

Thanks to our analysis we (i) developed a multifrequency classification scheme for hard X-ray sources, that can be later adopted also to investigate different high-energy surveys, (ii) investigate the main properties of sources populating the extragalactic hard X-ray sky and finally, extract other Seyfert galaxies now included in the 2nd release of the Turin-SyCAT catalog presented here.

We worked with the 1593 sources of the 3PBC catalog, comparing them with various other catalogs mentioned in the paper and adopting the following classification scheme criteria. Firstly, we checked if the 3PBC source has an assigned counterpart, if not, we performed multifrequency crossmatching analyses across the available literature to search for counterparts. Sources without counterparts were assigned with *unidentified* category. Those which were found with counterparts, together with sources already having a counterpart in the 3PBC catalog, were further inspected with multifrequency analyses. Sources

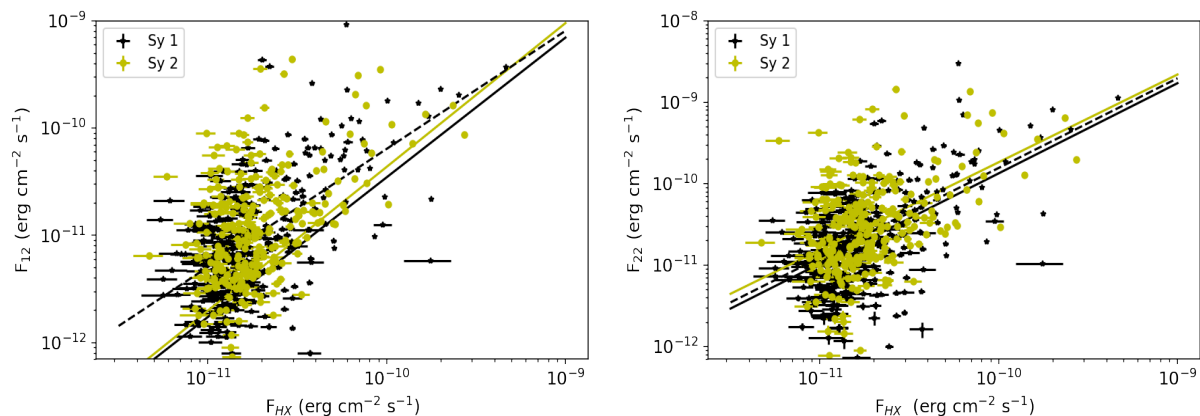


Fig. 16. Mid-IR fluxes at $12\ \mu\text{m}$ (Left panel) and $22\ \mu\text{m}$ (Right panel) as a function of hard X-rays flux. Regression lines were computed for the correlations between the W3 integrated flux and that in the hard X-ray band from the 3PBC, for both Seyfert 1 and 2 galaxies, marked in black and yellow, respectively. The dashed black line corresponds to the regression line computed for the whole sample while the straight black and yellow lines mark that for type 1 and type 2 Seyfert galaxies, respectively. The correlation coefficients are reported in Section 5.

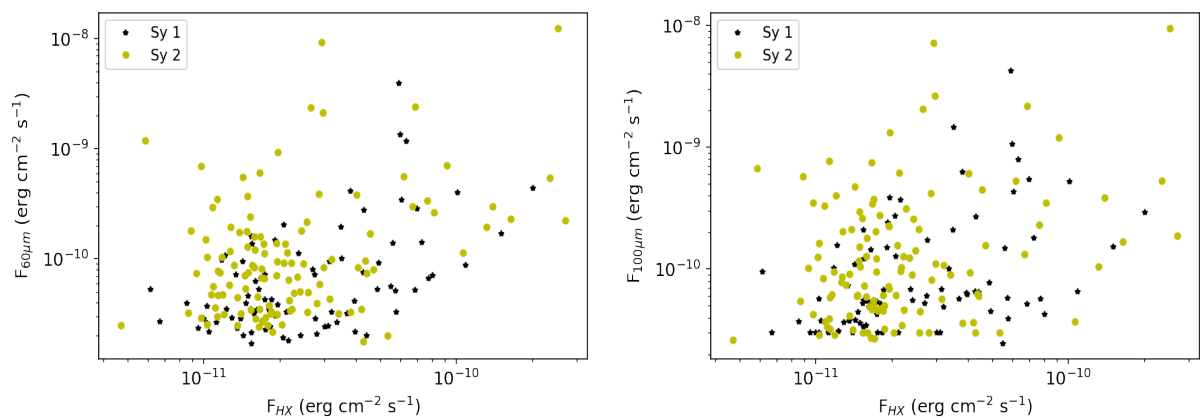


Fig. 17. Fluxes at $60\ \mu\text{m}$ (left panel) and $100\ \mu\text{m}$ (right panel) as a function of hard X-rays flux. Seyfert 1 and 2 galaxies are marked in black and yellow, respectively. No neat trend is evident between the two emissions.

lacking sufficient information to assign their class were put to *unclassified* category, the rest to *classified* category. We further distinguish the classified sources into Galactic and extragalactic and we purely focus on the extragalactic sources in this work.

Results obtained from our analysis can be outlined as follows.

1. The final revised 3PBC catalog we present in this study lists 1176 classified, 820 extragalactic, and 356 Galactic ones, 218 unidentified and 199 unclassified sources, respectively. The original version of the 3PBC catalog listed 244 unidentified and 362 unclassified sources counted according to our classification scheme (see Appendix for more details). We improved the fraction of 15.3% unidentified sources to 13.7% (from 244 to 218 sources) and the fraction of 22.7% unclassified sources to 12.5% (from 362 to 199 sources). It is important to highlight that 98 sources were classified in the original 3PBC catalog, but they were indeed listed as unclassified according to our refined analysis since they lacked multifrequency information.
2. The hard X-ray sky is mainly populated by nearby AGNs, where the two largest known populations of associated AGNs are: Seyfert galaxies ($\sim 79\%$) and blazars ($\sim 17\%$).

3. We report the trends between the hard X-ray and the gamma-ray emissions of those blazars that are also listed in the 4FGL as expected by the models widely adopted to explain their broadband SED.
4. In the presented 2^{nd} release of the Turin-SyCAT, we list 633 Seyfert galaxies, 282 new ones added here thus correspondent to increase their number by $\sim 80\%$ with respect to its 1^{st} release.
5. We updated the statistical analysis carried out comparing the hard X-ray and the IR emissions of Seyfert galaxies. All results obtained are in agreement with those previously found even if now the analysis appears more robust since it was performed with a sample of Seyfert galaxies increased by $\sim 80\%$ with respect to the 1^{st} release of the Turin-SyCAT.

Finally, we already checked the presence of SWIFT observations carried out using the X-ray telescope on board for the sample of unidentified hard X-ray sources and we found that more than 95% of them have at least a few ksec exposure time available. Thus the next step of the present analysis will be to search for the potential soft X-ray counterpart of these 3PBC unidentified sources to obtain their precise position necessary to carry out

optical spectroscopic campaigns aimed at identifying the whole sky seen between 15 and 150 keV.

Acknowledgements. We thank the anonymous referee for useful comments that led to improvements in the paper. M. K. and N. W. are supported by the GACR grant 21-13491X. E. B. acknowledges NASA grant 80NSSC21K0653. M. K. was supported by the Italian Government Scholarship issued by the Italian MAECI. VC acknowledges support from CONACyT research grants 280789 (Mexico). F. M. wishes to thank Dr. G. Cusumano for introducing him to the Palermo BAT Catalog project. We would like to thank A. Capetti for his work done on the 1st version of the Turin-SyCAT, which was relevant for this work. This investigation is supported by the National Aeronautics and Space Administration (NASA) grants GO0-21110X, GO1-22087X, and GO1-22112A. This research has made use of the NASA/IPAC Infrared Science Archive, which is funded by the National Aeronautics and Space Administration and operated by the California Institute of Technology. Funding for the Sloan Digital Sky Survey IV has been provided by the Alfred P. Sloan Foundation, the U.S. Department of Energy Office of Science, and the Participating Institutions. SDSS-IV acknowledges support and resources from the Center for High-Performance Computing at the University of Utah. The SDSS website is www.sdss.org. SDSS-IV is managed by the Astrophysical Research Consortium for the Participating Institutions of the SDSS Collaboration including the Brazilian Participation Group, the Carnegie Institution for Science, Carnegie Mellon University, Center for Astrophysics | Harvard & Smithsonian, the Chilean Participation Group, the French Participation Group, Instituto de Astrofísica de Canarias, The Johns Hopkins University, Kavli Institute for the Physics and Mathematics of the Universe (IPMU) / University of Tokyo, the Korean Participation Group, Lawrence Berkeley National Laboratory, Leibniz Institut für Astrophysik Potsdam (AIP), Max-Planck-Institut für Astronomie (MPIA Heidelberg), Max-Planck-Institut für Astrophysik (MPA Garching), Max-Planck-Institut für Extraterrestrische Physik (MPE), National Astronomical Observatories of China, New Mexico State University, New York University, University of Notre Dame, Observatório Nacional / MCTI, The Ohio State University, Pennsylvania State University, Shanghai Astronomical Observatory, United Kingdom Participation Group, Universidad Nacional Autónoma de México, University of Arizona, University of Colorado Boulder, University of Oxford, University of Portsmouth, University of Utah, University of Virginia, University of Washington, University of Wisconsin, Vanderbilt University, and Yale University. The Pan-STARRS1 Surveys (PS1) and the PS1 public science archive have been made possible through contributions by the Institute for Astronomy, the University of Hawaii, the Pan-STARRS Project Office, the Max-Planck Society, and its participating institutes, the Max Planck Institute for Astronomy, Heidelberg and the Max Planck Institute for Extraterrestrial Physics, Garching, The Johns Hopkins University, Durham University, the University of Edinburgh, the Queen's University Belfast, the Harvard-Smithsonian Center for Astrophysics, the Las Cumbres Observatory Global Telescope Network Incorporated, the National Central University of Taiwan, the Space Telescope Science Institute, the National Aeronautics and Space Administration under Grant No. NNX08AR22G was issued through the Planetary Science Division of the NASA Science Mission Directorate, the National Science Foundation Grant No. AST-1238877, the University of Maryland, Eotvos Lorand University (ELTE), the Los Alamos National Laboratory, and the Gordon and Betty Moore Foundation. This publication makes use of data products from the Wide-field Infrared Survey Explorer, which is a joint project of the University of California, Los Angeles, and the Jet Propulsion Laboratory/California Institute of Technology, funded by the National Aeronautics and Space Administration. TOPCAT and STILTS astronomical software (Taylor 2005) were used for the preparation and manipulation of the tabular data and the images.

References

Abazajian, K., Fuller, G. M., & Tucker, W. H. 2001, *ApJ*, 562, 593
 Abdo, A. A., Ackermann, M., Ajello, M., et al. 2010a, *ApJS*, 188, 405
 Abdo, A. A., Ackermann, M., Ajello, M., et al. 2010b, *ApJ*, 710, 810
 Abdollahi, S., Acero, F., Ackermann, M., et al. 2020, *ApJS*, 247, 33
 Abdurro'uf, Accetta, K., Aerts, C., et al. 2021, arXiv e-prints, arXiv:2112.02026
 Abell, G. O., Corwin, Harold G., J., & Olowin, R. P. 1989, *ApJS*, 70, 1
 Acharyya, A., Chadwick, P. M., & Brown, A. M. 2021, *MNRAS*, 500, 5297
 Ajello, M., Costamante, L., Sambruna, R. M., et al. 2009, *ApJ*, 699, 603
 Ajello, M., Greiner, J., Sato, G., et al. 2008, *ApJ*, 689, 666
 Ajello, M., Rebusco, P., Cappelluti, N., et al. 2010, *ApJ*, 725, 1688
 Antonucci, R. 1993, *ARA&A*, 31, 473
 Antonucci, R. R. J. & Miller, J. S. 1985, *ApJ*, 297, 621
 Ansfel, R. J., Stern, D., Kochanek, C. S., et al. 2013, *ApJ*, 772, 26
 Atwood, W. B., Abdo, A. A., Ackermann, M., et al. 2009, *ApJ*, 697, 1071
 Bade, N., Engels, D., Fink, H., et al. 1992, *A&A*, 254, L21
 Ballet, J., Burnett, T. H., Digel, S. W., & Lott, B. 2020, arXiv e-prints, arXiv:2005.11208

Balmaverde, B., Capetti, A., Marconi, A., et al. 2019, *A&A*, 632, A124
 Balmaverde, B., Capetti, A., Marconi, A., et al. 2021, *A&A*, 645, A12
 Bär, R. E., Trakhtenbrot, B., Oh, K., et al. 2019, *MNRAS*, 489, 3073
 Barthelmy, S. D. 2004, in *Society of Photo-Optical Instrumentation Engineers (SPIE) Conference Series*, Vol. 5165, X-Ray and Gamma-Ray Instrumentation for Astronomy XIII, ed. K. A. Flanagan & O. H. W. Siegmund, 175–189
 Baumgartner, W. H., Tueller, J., Markwardt, C. B., et al. 2013, *ApJS*, 207, 19
 Beckmann, V., Soldi, S., Shrader, C. R., Gehrels, N., & Produit, N. 2006, *ApJ*, 652, 126
 Bennett, C. L., Larson, D., Weiland, J. L., & Hinshaw, G. 2014, *ApJ*, 794, 135
 Bird, A. J., Barlow, E. J., Bassani, L., et al. 2004, *ApJ*, 607, L33
 Bird, A. J., Bazzano, A., Malizia, A., et al. 2016, *ApJS*, 223, 15
 Blandford, R. D. & Rees, M. J. 1978, in *BL Lac Objects*, ed. A. M. Wolfe, 328–341
 Blanton, M. R., Bershad, M. A., Abolfathi, B., et al. 2017, *AJ*, 154, 28
 Bock, D. C. J., Large, M. L., & Sadler, E. M. 1999, *AJ*, 117, 1578
 Bottacini, E., Ajello, M., & Greiner, J. 2012, *ApJS*, 201, 34
 Buttiglione, S., Capetti, A., Celotti, A., et al. 2010, *A&A*, 509, A6
 Cantó, J., Raga, A. C., & Rodríguez, L. F. 2000, *ApJ*, 536, 896
 Capetti, A., Axon, D. J., Macchetto, F. D., Marconi, A., & Winge, C. 1999, *ApJ*, 516, 187
 Capetti, A., Massaro, F., & Baldi, R. D. 2017a, *A&A*, 598, A49
 Capetti, A., Massaro, F., & Baldi, R. D. 2017b, *A&A*, 601, A81
 Cavaliere, A. & Setti, G. 1976, *A&A*, 46, 81
 Chambers, K. C., Magnier, E. A., Metcalfe, N., et al. 2016, arXiv e-prints, arXiv:1612.05560
 Charles, P. A. & Coe, M. J. 2003, arXiv e-prints, astro
 Churazov, E., Sunyaev, R., Revnivtsev, M., et al. 2007, *A&A*, 467, 529
 Comastri, A., Brusa, M., Ciliēgi, P., et al. 2002, arXiv e-prints, astro
 Condon, J. J., Cotton, W. D., Greisen, E. W., et al. 1998, *AJ*, 115, 1693
 Cowperthwaite, P. S., Massaro, F., D'Abrusco, R., et al. 2013, *AJ*, 146, 110
 Cusumano, G., La Parola, V., Segreto, A., et al. 2010, *A&A*, 524, A64
 Cutri, R. M., Wright, E. L., Conrow, T., et al. 2021, *VizieR Online Data Catalog*, II/328
 D'Abrusco, R., Álvarez Crespo, N., Massaro, F., et al. 2019, *ApJS*, 242, 4
 D'Abrusco, R., Massaro, F., Ajello, M., et al. 2012, *ApJ*, 748, 68
 D'Abrusco, R., Massaro, F., Paggi, A., et al. 2014, *ApJS*, 215, 14
 de Menezes, R., D'Abrusco, R., Massaro, F., Gasparrini, D., & Nemmen, R. 2020, *ApJS*, 248, 23
 Dermer, C. D. 1995, *ApJ*, 446, L63
 Diana, A., Caccianiga, A., Ighina, L., et al. 2022, *MNRAS*, 511, 5436
 Downes, R. A., Webbink, R. F., Shara, M. M., et al. 2005, *Journal of Astronomical Data*, 11, 2
 Edwards, R. T., Bailes, M., van Straten, W., & Britton, M. C. 2001, *MNRAS*, 326, 358
 Elvis, M., Civano, F., Vignali, C., et al. 2009, *ApJS*, 184, 158
 Elvis, M., Schreier, E. J., Tonry, J., Davis, M., & Huchra, J. P. 1981, *ApJ*, 246, 20
 Evans, P. A., Osborne, J. P., Beardmore, A. P., et al. 2014, *ApJS*, 210, 8
 Fanaroff, B. L. & Riley, J. M. 1974, *MNRAS*, 167, 31P
 Forman, W., Jones, C., Cominsky, L., et al. 1978, *ApJS*, 38, 357
 Frontera, F., Guidorzi, C., Montanari, E., et al. 2009, *ApJS*, 180, 192
 Frontera, F., Orlandini, M., Landi, R., et al. 2007, *ApJ*, 666, 86
 Gehrels, N., Chincarini, G., Giommi, P., et al. 2004, *ApJ*, 611, 1005
 Giacconi, R., Gursky, H., Paolini, F. R., & Rossi, B. B. 1962, *Phys. Rev. Lett.*, 9, 439
 Giacconi, R., Kellogg, E., Gorenstein, P., Gursky, H., & Tananbaum, H. 1971, *ApJ*, 165, L27
 Gilli, R., Comastri, A., & Hasinger, G. 2007, *A&A*, 463, 79
 Gilli, R., Risaliti, G., & Salvati, M. 1999, *A&A*, 347, 424
 Gilli, R., Salvati, M., & Hasinger, G. 2001, *A&A*, 366, 407
 Giodini, S., Pierini, D., Finoguenov, A., et al. 2009, *ApJ*, 703, 982
 Gower, J. F. R., Scott, P. F., & Wills, D. 1967, *MmRAS*, 71, 49
 Green, D. A. 1984, *MNRAS*, 209, 449
 Green, D. A. 2017, *VizieR Online Data Catalog*, VII/278
 Grimm, H. J., Gilfanov, M., & Sunyaev, R. 2002, *A&A*, 391, 923
 Gruber, D. E., Matteson, J. L., Peterson, L. E., & Jung, G. V. 1999, *ApJ*, 520, 124
 Güdel, M. & Nazé, Y. 2009, *A&A Rev.*, 17, 309
 Hales, S. E. G., Riley, J. M., Waldram, E. M., Warner, P. J., & Baldwin, J. E. 2007, *MNRAS*, 382, 1639
 Harrison, F. A., Aird, J., Civano, F., et al. 2016, *ApJ*, 831, 185
 Hasinger, G., Burg, R., Giacconi, R., et al. 1998, *A&A*, 329, 482
 Hasinger, G., Lehmann, I., Giacconi, R., et al. 1999, in *Highlights in X-ray Astronomy*, ed. B. Aschenbach & M. J. Freyberg, Vol. 272, 199
 Healey, S. E., Romani, R. W., Taylor, G. B., et al. 2007, *ApJS*, 171, 61
 Hilbert, B., Chiaberge, M., Kotyla, J. P., et al. 2016, *ApJS*, 225, 12
 Hine, R. G. & Longair, M. S. 1979, *MNRAS*, 188, 111
 Hovatta, T., Lister, M. L., Aller, M. F., et al. 2012, *AJ*, 144, 105
 Jarrett, T. H., Chester, T., Cutri, R., et al. 2000, *AJ*, 119, 2498

Table 6. Table of catalogs used in the cross-matching analysis.

Acronym	Catalogue Name	Reference
4FGL-DR2	The second release of the fourth <i>Fermi</i> -LAT catalog of γ -ray sources	1
3PBC	The 3 rd Palermo <i>Swift</i> -BAT Hard X-ray catalog	2
BAT105	The 105-month <i>Swift</i> -BAT catalog	3
<i>INTEGRAL</i>	The IBIS soft gamma-ray sky after 1000 <i>INTEGRAL</i> orbits	4
Homa-BZCAT	5 th edition of Roma-BZCAT catalog of blazars	5
3CR	The Revised Third Cambridge catalog	6
4C	The Fourth Cambridge Survey	7, 8
SyCAT	The Turin-SyCAT catalog	9
CVcat	The Catalog and Atlas of Cataclysmic Variables	10
SNRcat	The Catalog of Galactic Supernovae Remnants	11
hmbx	The 4 th edition of the catalog of High mass X-ray binaries in the Galaxy	12
lmbx	The 4 th edition of the catalog of Low mass X-ray binaries in the Galaxy and Magellanic Clouds	13
Rlmbx	The 7 th edition of the catalog of cataclysmic binaries, low mass X-ray binaries and related objects	14
ANTF	The Australian Telescope National Facility Pulsar Catalog	15
Abellcat	Abell catalog of rich galaxy clusters	16

References. (1) Ballet et al. (2020); (2) Cusumano et al. (2010); (3) Oh et al. (2018); (4) Bird et al. (2016); (5) Massaro et al. (2015a); (6) Spinrad et al. (1985); (7) Pilkington & Scott (1965); (8) Gower et al. (1967); (9) Peña-Herazo et al. (2022); (10) Downes et al. (2005); (11) Green (2017); (12) Liu et al. (2006); (13) Liu et al. (2007); (14) Ritter & Kolb (2003); (15) Manchester et al. (2005); (16) Abell et al. (1989).

- Jimenez-Gallardo, A., Massaro, F., Paggi, A., et al. 2021, *ApJS*, 252, 31
 Khachikian, E. E. & Weedman, D. W. 1971, *Astrofizika*, 7, 389
 Khachikian, E. Y. & Weedman, D. W. 1974, *ApJ*, 192, 581
 Knigge, C., Coe, M. J., & Podsiadlowski, P. 2011, *Nature*, 479, 372
 Kollatschny, W. & Zetzl, M. 2013, *A&A*, 549, A100
 Koss, M., Trakhtenbrot, B., Ricci, C., et al. 2017, *ApJ*, 850, 74
 Koss, M., Trakhtenbrot, B., Ricci, C., et al. 2019, in *American Astronomical Society Meeting Abstracts #233*, 431.04
 Kotyla, J. P., Chiaberge, M., Baum, S., et al. 2016, *ApJ*, 826, 46
 Krivonos, R., Revnivtsev, M., Lutovinov, A., et al. 2007, *A&A*, 475, 775
 Krivonos, R., Wik, D., Grefenstette, B., et al. 2021a, *MNRAS*, 502, 3966
 Krivonos, R. A., Bird, A. J., Churazov, E. M., et al. 2021b, *New A Rev.*, 92, 101612
 Krivonos, R. A., Sazonov, S. Y., Kuznetsova, E. A., et al. 2022, *MNRAS*, 510, 4796
 Krivonos, R. A., Tsygankov, S. S., Mereminskiy, I. A., et al. 2017, *MNRAS*, 470, 512
 Landi, R., Bassani, L., Bazzano, A., et al. 2017, *MNRAS*, 470, 1107
 Landoni, M., Massaro, F., Paggi, A., et al. 2015, *AJ*, 149, 163
 Law, C. & Yusef-Zadeh, F. 2004, *ApJ*, 611, 858
 Lebrun, F., Leray, J. P., Lavocat, P., et al. 2003, *A&A*, 411, L141
 Levine, A. M., Lang, F. L., Lewin, W. H. G., et al. 1984, *ApJS*, 54, 581
 Liu, Q. Z., van Paradijs, J., & van den Heuvel, E. P. J. 2006, *A&A*, 455, 1165
 Liu, Q. Z., van Paradijs, J., & van den Heuvel, E. P. J. 2007, *A&A*, 469, 807
 Madrid, J. P., Chiaberge, M., Floyd, D., et al. 2006, *ApJS*, 164, 307
 Malizia, A., Bassani, L., Sguera, V., et al. 2010, *MNRAS*, 408, 975
 Malizia, A., Landi, R., Molina, M., et al. 2016, *MNRAS*, 460, 19
 Manchester, R. N., Hobbs, G. B., Teoh, A., & Hobbs, M. 2005, *AJ*, 129, 1993
 Manchester, R. N., Lyne, A. G., Camilo, F., et al. 2001, *MNRAS*, 328, 17
 Maraschi, L., Fossati, G., Tavecchio, F., et al. 1999, *ApJ*, 526, L81
 Maraschi, L., Ghisellini, G., & Celotti, A. 1992, *ApJ*, 397, L5
 Marchesini, E. J., Masetti, N., Palazzi, E., et al. 2019, *Ap&SS*, 364, 153
 Markwardt, C. B., Tueller, J., Skinner, G. K., et al. 2005, *ApJ*, 633, L77
 Marscher, A. P. & Gear, W. K. 1985, *ApJ*, 298, 114
 Maselli, A., Massaro, F., Cusumano, G., et al. 2016, *MNRAS*, 460, 3829
 Masetti, N., Mason, E., Morelli, L., et al. 2008, *A&A*, 482, 113
 Masetti, N., Morelli, L., Palazzi, E., et al. 2006, *A&A*, 459, 21
 Masetti, N., Parisi, P., Jiménez-Bailón, E., et al. 2012, *A&A*, 538, A123
 Masetti, N., Parisi, P., Palazzi, E., et al. 2013, *A&A*, 556, A120
 Masetti, N., Parisi, P., Palazzi, E., et al. 2009, *A&A*, 495, 121
 Massaro, E., Giommi, P., Leto, C., et al. 2009, *A&A*, 495, 691
 Massaro, E., Maselli, A., Leto, C., et al. 2015a, *Ap&SS*, 357, 75
 Massaro, F. & D'Abrusco, R. 2016, *ApJ*, 827, 67
 Massaro, F., D'Abrusco, R., Ajello, M., Grindlay, J. E., & Smith, H. A. 2011, *ApJ*, 740, L48
 Massaro, F., D'Abrusco, R., Landoni, M., et al. 2015b, *ApJS*, 217, 2
 Massaro, F., D'Abrusco, R., Paggi, A., et al. 2013a, *ApJS*, 209, 10
 Massaro, F., D'Abrusco, R., Tosti, G., et al. 2012a, *ApJ*, 750, 138
 Massaro, F., D'Abrusco, R., Tosti, G., et al. 2012b, *ApJ*, 752, 61
 Massaro, F., Harris, D. E., Liuzzo, E., et al. 2015c, *ApJS*, 220, 5
 Massaro, F., Harris, D. E., Tremblay, G. R., et al. 2010, *ApJ*, 714, 589
 Massaro, F., Harris, D. E., Tremblay, G. R., et al. 2013b, *ApJS*, 206, 7
 Massaro, F., Masetti, N., D'Abrusco, R., Paggi, A., & Funk, S. 2014, *AJ*, 148, 66
 Massaro, F., Paggi, A., Errando, M., et al. 2013c, *ApJS*, 207, 16
 Massaro, F., Tremblay, G. R., Harris, D. E., et al. 2012c, *ApJS*, 203, 31
 Mauch, T., Murphy, T., Buttery, H. J., et al. 2003, *MNRAS*, 342, 1117
 Mereminskiy, I. A., Krivonos, R. A., Lutovinov, A. A., et al. 2016, *MNRAS*, 459, 140
 Mirabel, I. F. 2010, in *Lecture Notes in Physics*, Berlin Springer Verlag, ed. T. Belloni, Vol. 794, 1
 Missaglia, V., Massaro, F., Liuzzo, E., et al. 2021, *ApJS*, 255, 18
 Miyaji, T., Wilson, A. S., & Perez-Fourmon, I. 1992, *ApJ*, 385, 137
 Moffet, A. T. 1966, *ARA&A*, 4, 145
 Molina, M., Bassani, L., Malizia, A., et al. 2009, *MNRAS*, 399, 1293
 Nevalainen, J., Lieu, R., Bonamente, M., & Lumb, D. 2003, *ApJ*, 584, 716
 Oh, K., Koss, M., Markwardt, C. B., et al. 2018, *ApJS*, 235, 4
 Oskinova, L. M. 2005, *MNRAS*, 361, 679
 Paiano, S., Falomo, R., Treves, A., & Scarpa, R. 2020, *MNRAS*, 497, 94
 Paiano, S., Landoni, M., Falomo, R., Treves, A., & Scarpa, R. 2017, *ApJ*, 844, 120
 Paliya, V. S., Koss, M., Trakhtenbrot, B., et al. 2019, *ApJ*, 881, 154
 Parisi, P., Masetti, N., Rojas, A. F., et al. 2014, *A&A*, 561, A67
 Peña-Herazo, H. A., Marchesini, E. J., Álvarez Crespo, N., et al. 2017, *Ap&SS*, 362, 228
 Peña-Herazo, H. A., Massaro, F., Chavushyan, V., et al. 2019, *Ap&SS*, 364, 85
 Peña-Herazo, H. A., Massaro, F., Chavushyan, V., et al. 2022, *A&A*, 659, A32
 Pilkington, J. D. H. & Scott, J. F. 1965, *MNRAS*, 69, 183
 Privon, G. C., O'Dea, C. P., Baum, S. A., et al. 2008, *ApJS*, 175, 423
 Revnivtsev, M., Molkov, S., & Sazonov, S. 2006, *MNRAS*, 373, L11
 Revnivtsev, M., Sazonov, S., Krivonos, R., Ritter, H., & Sunyaev, R. 2008, *A&A*, 489, 1121
 Ricci, C., Trakhtenbrot, B., Koss, M. J., et al. 2017, *ApJS*, 233, 17
 Ricci, F., Massaro, F., Landoni, M., et al. 2015, *AJ*, 149, 160
 Ritter, H. & Kolb, U. 2003, *A&A*, 404, 301
 Rodriguez Espinosa, J. M., Rudy, R. J., & Jones, B. 1987, *ApJ*, 312, 555
 Rojas, A. F., Masetti, N., Minniti, D., et al. 2017, *A&A*, 602, A124

- Rothschild, R., Boldt, E., Holt, S., et al. 1979, *Space Science Instrumentation*, 4, 269
- Sarazin, C. L. 1986, *Reviews of Modern Physics*, 58, 1
- Sazonov, S., Revnivtsev, M., Krivonos, R., Churazov, E., & Sunyaev, R. 2007, *A&A*, 462, 57
- Schmidt, M. 1969, *ARA&A*, 7, 527
- Searle, L., Sargent, W. L. W., & Bagnuolo, W. G. 1973, *ApJ*, 179, 427
- Segreto, A., Cusumano, G., Ferrigno, C., et al. 2010, *A&A*, 510, A47
- Seyfert, C. K. 1943, *ApJ*, 97, 28
- Singh, R., van de Ven, G., Jahnke, K., et al. 2013, *A&A*, 558, A43
- Skrutskie, M. F., Cutri, R. M., Stiening, R., et al. 2006, *AJ*, 131, 1163
- Smith, K. L., Mushotzky, R. F., Koss, M., et al. 2020, *MNRAS*, 492, 4216
- Spinrad, H., Djorgovski, S., Marr, J., & Aguilar, L. 1985, *PASP*, 97, 932
- Stickel, M., Padovani, P., Urry, C. M., Fried, J. W., & Kuehr, H. 1991, *ApJ*, 374, 431
- Stuardi, C., Missaglia, V., Massaro, F., et al. 2018, *ApJS*, 235, 32
- Taylor, J. H., Manchester, R. N., & Lyne, A. G. 1993, *ApJS*, 88, 529
- Taylor, M. B. 2005, in *Astronomical Society of the Pacific Conference Series*, Vol. 347, *Astronomical Data Analysis Software and Systems XIV*, ed. P. Shopbell, M. Britton, & R. Ebert, 29
- Tueller, J., Mushotzky, R. F., Barthelmy, S., et al. 2008, *ApJ*, 681, 113
- Ubertini, P., Lebrun, F., Di Cocco, G., et al. 2003, *A&A*, 411, L131
- Ueda, Y., Akiyama, M., Hasinger, G., Miyaji, T., & Watson, M. G. 2014, *ApJ*, 786, 104
- Urry, C. M. & Padovani, P. 1995, *PASP*, 107, 803
- Valinia, A. & Marshall, F. E. 1998, *ApJ*, 505, 134
- van Velzen, S., Falcke, H., Schellart, P., Nierstenhöfer, N., & Kampert, K.-H. 2012, *A&A*, 544, A18
- Vaona, L., Ciroi, S., Di Mille, F., et al. 2012, *MNRAS*, 427, 1266
- Vink, J. 2012, *A&A Rev.*, 20, 49
- Voges, W., Aschenbach, B., Boller, T., et al. 1999, *A&A*, 349, 389
- Warner, B. 1995, *Cataclysmic variable stars*, Vol. 28
- Weedman, D. W. 1977, *ARA&A*, 15, 69
- Weedman, D. W., Feldman, F. R., Balzano, V. A., et al. 1981, *ApJ*, 248, 105
- Weisskopf, M. C., Tananbaum, H. D., Van Speybroeck, L. P., & O'Dell, S. L. 2000, in *Society of Photo-Optical Instrumentation Engineers (SPIE) Conference Series*, Vol. 4012, *X-Ray Optics, Instruments, and Missions III*, ed. J. E. Truemper & B. Aschenbach, 2–16
- Winkler, C., Courvoisier, T. J. L., Di Cocco, G., et al. 2003, *A&A*, 411, L1
- Wolter, A., Beckmann, V., Ghisellini, G., Tavecchio, F., & Maraschi, L. 2008, in *Astronomical Society of the Pacific Conference Series*, Vol. 386, *Extragalactic Jets: Theory and Observation from Radio to Gamma Ray*, ed. T. A. ReCTOR & D. S. De Young, 302
- Yuan, F. & Narayan, R. 2004, *ApJ*, 612, 724

Appendix A: Re-classification of the original 3PBC based on our classification scheme

We compare our refined classification for the counterparts of 3PBC sources with those previously assigned in the original catalog. To perform this, we first “translate” the original 3PBC classes into our classification scheme according to the following criteria. For the Galactic objects we consider (i) all sources classified in the original 3PBC as HXB, LXB, XB, XB*, V* being indicated as “bin” (i.e., binary systems); (ii) those previously labeled as AM*, CV, CV*, DN*, DQ*, EB*, NL*, No currently belong to the “cv” class (i.e., cataclysmic variables); while (iii) those few classified as Psr are all “psr”, SNR is “snr” and PN simply “pn” (i.e., pulsars, supernova remnants, and planetary nebulae, respectively). On the other hand, for the extragalactic classes: (i) sources labeled as BLA and BZC in the original 3PBC are indicated as “blz” (i.e., blazars); (ii) Sy*, SyG, Sy1, Sy2 are all classified as “sey” according to our scheme (i.e., Seyfert galaxies) while (iii) QSO are “qso” and rG is “rdg” (i.e., being quasars and radio galaxies respectively) and then (iv) objects classified as LIN and CIG are now indicated as “liner” and “clu”, respectively being LINERs and galaxy clusters. The remaining handful of sources had the same classification in both lists, for example, the Galactic center.

For the unknown sources, we considered those having a question mark in the classification label, remarking that this could be unsettled, as well as those indicated as AGN, BRT, EmG, G, GiC, GiP, IG, IR, X, gam and Rad, all “unc”. This is because even if for example the associated counterpart in the original 3PBC is recognized as an infrared or an X-ray source, or a simple AGN, this does not provide us precise information about its nature and its hard X-ray emission. Finally, 3PBC sources originally lacking an assigned counterpart were all labeled as “uhx”, being unidentified hard X-ray sources.

In Table A.1 we report the (i) 3PBC name, (ii) the original 3PBC classification, (iii) the new label corresponding to our new classification scheme but assigned on the basis of the previous criteria and on the information available before our refined analysis and (iv) our new classification based on the multifrequency analysis carried out here. This allowed us to compare previous and new associations and classifications to obtain an estimate of the improvements achieved.

We found that, according to our classification scheme, the 3PBC catalog presented 521 Seyfert galaxies, 109 blazars, 362 unclassified sources, and 244 unidentified sources. In our revised version of the 3PBC, we present 593 Seyfert galaxies, 129 blazars, 199 unclassified sources, and 218 unidentified sources. It is important to highlight, that due to our classification criteria, we not only classified some of the yet unclassified or unidentified sources, but we also re-classified 98 sources that had a classification class in the original 3PBC, as unclassified according to our classification criteria. This was done in cases of a lack of information in the literature, e.g. if we could not find an optical spectrum or luminosities, etc.

Table A.1. The comparison between the original classes assigned in the 3PBC, how they are interpreted according to our new scheme and that obtained thanks to our refined analysis, for all 3PBC sources. For each source, we report the following columns: (i) the 3PBC name; (ii) the original class; (iii) the class interpreted according to our scheme; (iv) the class assigned in our refined analysis.

name_3PBC	class3PBC	reclass	class	subclass
J0000.9-0708	X	unc	sey	sy2
J0001.7-7659	G	unc	sey	sy1
J0002.5+0322	Sy1	sey	sey	sy1
J0003.4+2738	G	unc	sey	sy2
J0004.0+7018	AG?	unc	sey	sy2